東京大学　大学院新領域創成科学研究科
基盤科学研究系
先端エネルギー工学専攻

平成18年度

修士論文

Numerical method for analyzing the scale hierarchy of plasmas based on smoothed particle hydrodynamics

(SPH法に基づいたマルチスケールシミュレーション法の開発)

2007年2月提出
指導教員　吉田　善章　教授

46209　沼澤　修平

Contents

Chapter 1

Introduction

The dynamics of plasma is characterized by the interactions of widely separated space/time scales, that is, the behavior of macroscale phenomena is intrinsically coupled to and induced by the dynamics at the microscopic scales. In the most microscopic scale within the classical mechanics, the dynamics is characterized by individual particles' motion. Charged particles, typically ions and electrons, move in the self-consistent electromagnetic fields. Charged particles evolve with gyration around magnetic field lines, successive collisions and interactions with waves. On the other hand, in the macroscopic view, the plasma is understood as an electrically conducting fluid and the length scale is related to the whole system, such as a length of a confinement device in the laboratory plasma and a size of a plasma in the astrophysical environment. Scale hierarchy is created in the dynamics of plasma and each level of the hierarchy interacts with different levels of it. Multiscale phenomena are observed in several research fields, both laboratory and astrophysical plasmas.

A model is constructed to capture a dominant characterics for a phenomenon. In the case of plasma physics, we can provide a lot of models corresponding to some level of the scale hierarchy. Thus necessarily the models also create a hierarchy. Before proceeding the discussion about the coupling between macro and microscales, let us touch on the hierarchy of models, that is, how to understand each level of the scale hierarchy.

A schematic view of the hierarchy of model equations is shown in Fig. 1.1. The most microscopic description of the plasma is that we consider a system as a collection of charged particles, following the Newton's equation

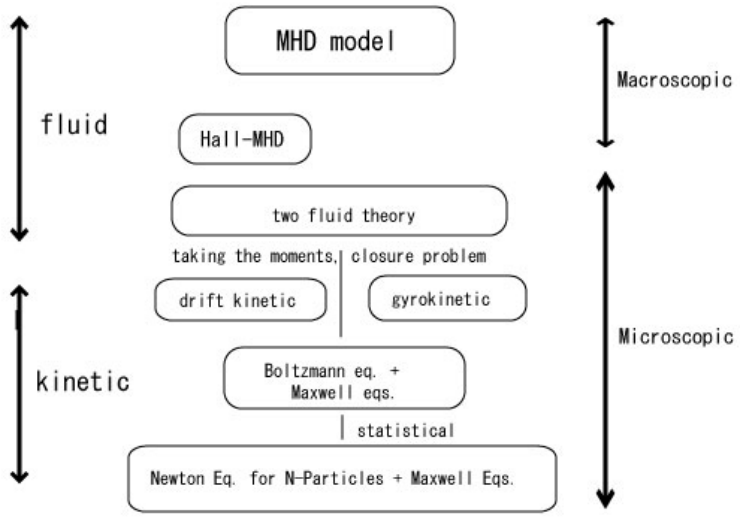

Figure 1.1: A schematic picture of the hierarchy of model equations describing the dynamics of plasma.

of motion. In terms of this model, we have to solve the same number of equations as particles and Maxwell's equations. For example, The number of equations related to the equation of motion is of the order of 10^{20} for the typical magnetic fusion plasma. In principle, we can solve them numerically, but it is bad for a theoretical insight. Thus we introduce a statistical description of plasmas, and the model is called "kinetic theory".

In the kinetic theory, a state is described by the distribution function $f(\boldsymbol{x}, \boldsymbol{v}, t)$. The distribution fuction $f(\boldsymbol{x}, \boldsymbol{v}, t)$ is a funciton of spatial coordinate $\boldsymbol{x}$, velocity $\boldsymbol{v}$, and time t, where $f(\boldsymbol{x}, \boldsymbol{v}, t)d^3xd^3v$ denotes a number of particles in the six-dimensional volume element d^3xd^3v centered at $(\boldsymbol{x}, \boldsymbol{v})$. A time development of a system is governed by the Boltzmann equation and the Maxwell's equations. Based on the kinetic theory, we can obtain some models corresponding to physical situations, such as magnetized or non-magnetized, and collisional or collisionless. For example, when a plasma is magnetized, a Larmor-radius r_L is much smaller than a system length L. Then, we can separate the scale of gyromotion and the plasma is described in terms of guiding center variables. This model is called "gyrokinetic" or "drift kinetic" depending on an assumption whether we neglect a small perturbative component of the electromagnetic field. Another example is a case when a plasma is collisional. In that case we are able to describe the plasma in terms of a fluid description by taking velocity moments, or averaging over the velocity space, of the Boltzmann equation. [1](The details of the calculation of velocity moments is written in various text books. It was originally proposed by Chapman and Cowling [3] and Braginskii [4]). The resultant model is called "two-fluid theory". The concrete form of equations are listed in Chapter 2. This model cannot capture the individual particle effect, but it still contains microscopic time/space scales, such as the plasma frequency and the gyro-frequency. The difference between electron fluid's motion and ion fluid's motion allow a variety of structures and dynamics of the order of the intrinsic length/time scale of each fluid.

When we get rid of microscopic scales from two-fluid theory, we can construct the macroscopic description of the plasma. The model is called "Magnetohydrodynamics (MHD)". MHD theory is valid for the dynamics involving the whole system scale. Since MHD is simpler than other models, it have

[1]This reduction of the model is related to the classical "closure problem". "Closure problem" can be inferred as how to get rid of microscopic scale rigorously.

been mainly analyzed in the long history of plasma physics. As we showed here, a model corresponding to each level of the scale hierarchy is acquired by scale separation which average out the dynamical effects dominated in the smaller scale we pay attention to.

Here let me discuss the scale coupling between micro- and macro-scales again with an illustrative example, magnetic reconnection. Magnetic reconnction is a fundamental process which allows magnetized plasmas to convert the energy stored in the magnetic fields into kinetic energy of the plasma. It plays an important role in the dynamics of space and laboratory plasmas. At the magnetopause, magnetic reconnection allows particles from the solar wind to enter the magnetosphere. Also it is believed to be the main source of energy for solar flares and coronal mass ejections.

In ideal MHD, a model which neglects the classical resistivity and having some global conservation laws, the frozen-in flux condition prohibits a change of the magnetic field topology. Thus reconnection depends on a mechanism that breaks the frozen-in condition. This nonideal mechanism is responsible for the dynamics in the diffusion region, where the topology change takes place. In resistive MHD with uniform resistivity an elongated Sweet-Parker current sheet develops, however, the reconnection rate, which is the rate of flux change, obtained from Sweet-Parker model is too much small to assure the observed reconnection rate [5,6].

Currently it has become apparent that we have to employ Hall-MHD model at least to adequately describe collisionless reconnection [29]. The microscopic structure, of the order of the ion skin depth, generated by the Hall-effect enhances the reconnection process. Here, the ion skin depth λ_i is a characteristic length provided by the Hall effect. Therefore, a comprehensive treatment, which takes into account microscopic dynamics of the order of the ion skin depth, is necessary for the reconnection problem.

As we see from Table 1.1, in the case of solar flares, the system size is 10^8 times greater than the ion skin depth. Although computer simulation is becoming a powerful tool for studying plasma physics as computational capability progresses, it is difficult to handle problems that have considerably distinct scales. Theoretically, we have treated them in a framework of "singular perturbation". Singular perturbation is defined as a perturbation which changes the largest order of a differential operator. In the context of

Table 1.1: Characteristic spatial scales of the solar coronal plasma in SI unit.

solar radius	R	7×10^9
active regions	L	10^8
ion skin depth	c/ω_i	10^1
electron skin depth	c/ω_e	10^{-1}
ion Larmor radius	$r_{L,i}$	10^{-1}
electron Larmor radius	ρ_e	10^{-3}
Debye length	λ_D	10^{-3}

physics, typically it is expressed by a product of a small coefficient ϵ and the higher order derivative. The heart of the singular perturbations is a connection between the global structure and an intrinsic structure dominated by the singular perturbation in a localized singular region.

The resistivity term and the Hall term are treated as singular perturbation for ideal MHD equations. Particularly, it is proposed in the two-fluid relaxation theory that the double Beltrami field is expressed by a combination of two different Beltrami fields (eigenfunctions of the curl operator). The double Beltrami field has two scale length, and can deal with the different scale interaction. For example, one is a large scale determined by the macroscopic structure, while the other is the intrinsic scale of the order of the ion skin depth [9].

Nowadays a development of a multiscale simulation algorhithm is an attractive study field for plasma physicists. There seems to be two types of ideas. First one is that a macroscopic structure of a system is extrapolated from the microscopic structure. "Equation free" method and "Integrative projection" method are contained in this framework. The other resembles the singular perturbation, that is a connection between a macroscopic structure described by the macroscopic model and a microscopic structure in terms of the microscopic model. A typical example of this notion is MHD-PIC code, developed by the group of the Earth Simulator Center. They aim to simulate the reconnection physics precisely. Microscopic dynamics in the diffusion region is simulated in terms of PIC code which is capable of capturing the kinetic effects and the macroscopic structure in the outer region, surrounding the diffusion region, is treated by MHD (See Fig. 1.2, [30]). In their numerical scheme, the physical quantities are defiend on grids spreading over

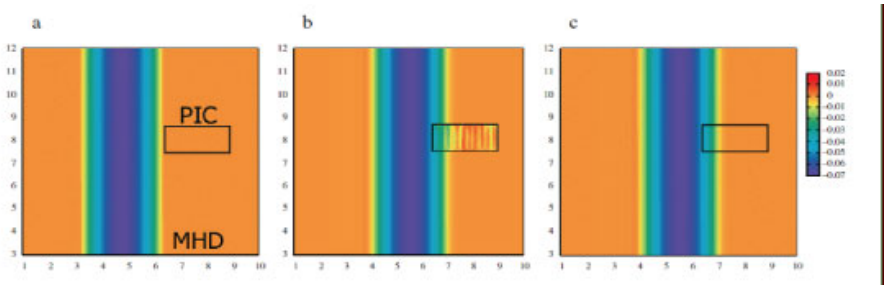

Figure 1.2: The test simulation of the MHD-PIC interlocked model developed by the multiscale algorithm group of the Earth Simulator Center [30].

a computational domain in both MHD and PIC regions. Basic equations corresponding to each grid is obtained by discretization of the conservative form of the partial differential equations which are originated from a concept that the field is understood as Eulerian variables. Therefore their study can be recognized as a development of singular-perturbation-like multiscale algorithm in terms of Eulerian variables. The study of multiscale simulation was just started, thus we have a sufficent scope to construct a new approach to it in a different manner.

Here we consider a new multiscale simulation algorithm. Coupling of different scales in a simulation scheme is performed well in terms of Lagrange description of the field variables at each level of the scale hierarchy. The reason is as follows. In terms of the Lagrange description, time development of a model equation is characterized by the velocity $\boldsymbol{v}$, that is, the velocity constructs a characteristic curve. Altough the meaning of the velocity is changed in each level of the scale hierarchy, for example, in the microscopic scale $\boldsymbol{v}$ expresses the velocity of a particle, while on the other hand in the macroscopic model $\boldsymbol{v}$ stands for the flow of an electrically conducting fluid. The idea of the velocity penetrates the model hierarchy from the macroscopic MHD model to the microscopic kinetic theory. This gives a coherent discipline for a multiscale system and may work efficiently for the coupling of different scales. The Lagrange description of the field corresponds to the (quasi-) particle method in the simulation and the multiscale simulation in terms of particle method is understood schematically as Fig. 1.3.

A quasi-particle moves in the computational domain and changes its property corresponding to the enviroment where it moves. The environment itself

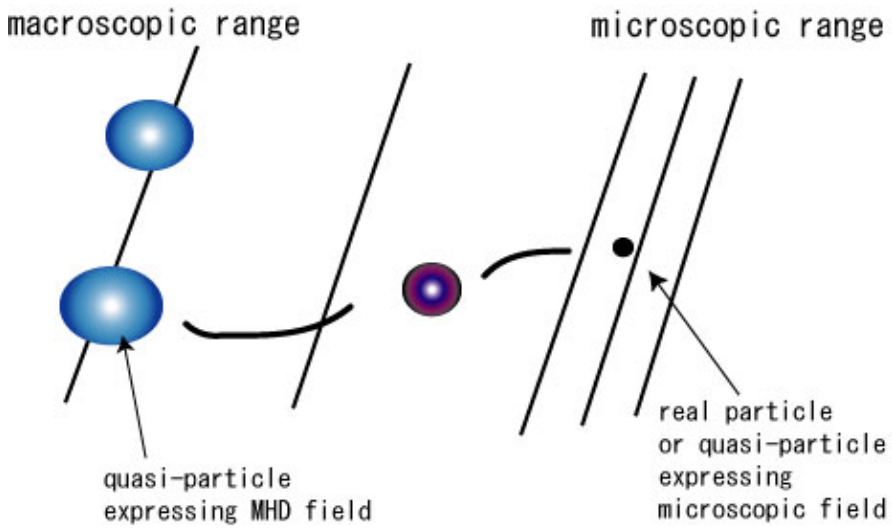

Figure 1.3: Schematic view of a multiscale particle method: a quasi-particle moves in a system with changing the property depending on the enviroment. The environment itself is governed by the motion of the quasi-particles.

is governed by the motion of the quasi-particles. In the macroscopic area, the particle expresses the MHD-characteristics and if the particle goes into the area where microscopic effects should be considered, the particle changes its property as expressing the real particle effect. We call this idea of multiscale simulation based on the particle view as "multiscale (quasi-)particle simulation".

Thus, in my thesis, I investigate basic features of multiscale partice simulation. Particularly, I study the scale coupling between MHD model and two-fluid model. In Chap. 2, I investigate the connection between MHD model and two-fluid model theoretically. The algebraic connection between MHD and two-fluid model is well understood, that is, we can derive MHD model from two-fluid model by scale separation of microscopic effects (dicussed in Sec. 2.1). However, their connection in terms of Lagrangian formulation or variational principle has not been clarified. We will see that the MHD equation of motion is derived from a two-fluid Lagrangian extended from the Lagrangian of a particle in Sec. 2.3. Our Lagrangian and the following variational principle is based on a fact that plasmas are constituted by charged

particles. This point is often ignored in the MHD model. The connection in terms of the Lagrangian constructed by a particle (Lagrange) view can be translated as follows. The Lagrange view is essential to the scale coupling, and this supports the philosophy of multiscale particle simulation.

In Chap. 3, We describe how to develop a numerical scheme of Hall-MHD, the fluid model containing microscopic effects. We apply Smoothed Particle Hydrodynamics (SPH) method to the Hall-MHD model. SPH is developed in the fluid dynamics and it is known that model equations for the numerical scheme is derived from the variational principle. By this knowledge, SPH is deeply related to the principles of mechanics and seems to be suitable for the multiscale particle simulation. Since the SPH method for MHD model has been developed already, if we develop a SPH method for Hall-MHD model, the tool for the multiscale fluid simulation in terms of SPH will be prepared.

The conventional SPH with a focus on the main concept of it is introduced in Sec. 3.1. Quasi-particles expressing the two-fluid model can not avoid the gyro-motion due to the electromagnetic force $\boldsymbol{v} \times \boldsymbol{B}$. This gyromotion prevents us from capturing the fluid motion of interest and in numerically makes difficult to obtain a large time step. Thus, we develop a reduced Hall-MHD model by utilizing drift approximation, it is stated in Sec. 3.2. In terms of the developed numerical scheme, we simulate shear Alfvén wave as a representive example of transverse wave and obtain a dispersion relation numerically. Although quasi particles do not move along the magnetic field lines, the wave motion along the magnetic field lines is well obtained. In this case, quasi-particles can behave as fixed grids used in numerical schemes based on finite difference. The numerical results agree well with the dispersion relation obtained analytically.

In Chap. 4, we develop a SPH method coupled with the Poisson's equation. In the Hall-MHD SPH scheme using the drift approximation, we do not capture the motion along the magnetic field. A driver of tangential motion is the pressure, which is the apparent difference between quasi-particles and real particles. Thus checking whether the SPH scheme can simulate the pressure effect precisely is an important task. The model equations and the algorithm are shown in Sec. 4.2 - 4.4. In terms of the developed SPH numerical scheme, we simulate one-dimensional electron plasma (Langmuir) wave as an example of electrostatic longitudinal waves, in cotrast to the shear

Alfvén wave discussed in Chap. 2. We obtain a dispersion relation of Langmuir wave numerically, which agrees well with the dispersion relation derived analytically.

In Chap. 5, I simulate a propagation of a nonlinear wave, particularly an ion acoustic soliton. Fundamental properties for ion acoustic wave is same as the case for Langmuir wave. This simulation assures that the numerical scheme works well in the nonlinear regime. I introduce a theoretical treatment of the ion acoustic soliton in Sec. 5.1. The model equations for numerical scheme is shown in Sec. 5.2. I simulate two cases: linear dispersion relation of ion acoustic wave and traveling of non-linear ion acoustic soliton. The results are stated in Sec. 5.4.

In Chap. 6, I will summarize the results and give conclusions.

Chapter 2

Relations between two-fluid model and MHD model

2.1 Algebraic relation

In this chapter, We investigate the relation between two-fluid model and MHD model. The reason why we investigate the relation is that we should know the relation of them deeply to connect them in a numerical scheme. Particularly, we see a relationship of variational principles between MHD model and two-fluid model. The variational principles is one of the frameworks of mechanics and employed in the most of fields of physics. Before proceeding to the discussion about variational principles, we mention the algebraic connection of them, since the algebraic relation between MHD and two-fluid model relates the relation between them in the context of the variational principles.

MHD model is derived by approximations which neglect high-frequency and short-wavelength motion from two-fluid model.

We start with the two-fluid model of plasmas. As already introduced in Chap. 1, the two-fluid model is obtained by taking velocity moments of the Boltzmann equation or integration over the velocity space. First three

moments are shown as

$$\frac{\partial n_i}{\partial t} = -\nabla \cdot (n_i \boldsymbol{u}_i), \tag{2.1a}$$

$$\frac{\partial n_e}{\partial t} = -\nabla \cdot (n_e \boldsymbol{u}_e), \tag{2.1b}$$

$$m_i n_i \left\{ \frac{\partial \boldsymbol{u}_i}{\partial t} + (\boldsymbol{u}_i \cdot \nabla)\boldsymbol{u}_i \right\} = e n_i (\boldsymbol{E} + \boldsymbol{u}_i \times \boldsymbol{B}) - \nabla p_i - \nabla \cdot \boldsymbol{\pi}_i - \boldsymbol{R}, \tag{2.1c}$$

$$m_e n_e \left\{ \frac{\partial \boldsymbol{u}_e}{\partial t} + (\boldsymbol{u}_e \cdot \nabla)\boldsymbol{u}_e \right\} = -e n_e (\boldsymbol{E} + \boldsymbol{u}_e \times \boldsymbol{B}) - \nabla p_e - \nabla \cdot \boldsymbol{\pi}_e + \boldsymbol{R}, \tag{2.1d}$$

$$\frac{3}{2} \left\{ \frac{\partial p_i}{\partial t} + (\boldsymbol{u}_i \cdot \nabla) p_i \right\} + \frac{5}{2} p_i \nabla \cdot \boldsymbol{u}_i = -\nabla \cdot \boldsymbol{q}_i - \boldsymbol{\pi}_i : \nabla \boldsymbol{u}_i + Q_i, \tag{2.1e}$$

$$\frac{3}{2} \left\{ \frac{\partial p_e}{\partial t} + (\boldsymbol{u}_e \cdot \nabla) p_e \right\} + \frac{5}{2} p_e \nabla \cdot \boldsymbol{u}_e = -\nabla \cdot \boldsymbol{q}_e - \boldsymbol{\pi}_e : \nabla \boldsymbol{u}_e + Q_e, \tag{2.1f}$$

where, $n_{e,i}$ are the number densities, $\boldsymbol{u}_{e,i}$ are the flow velocities, $p_{e,i}$ are the pressures, $m_{e,i}$ are the masses, $\boldsymbol{\pi}_{e,i}$ are the viscous stress tensors, $\boldsymbol{R}$ is the momentum transfer between electrons and ions, $\boldsymbol{q}_{e,i}$ are the heat flows, $Q_{e,i}$ are the heat generated due to collisions of each fluid and e is the elementary charge. The equality

$$p_{e,i} = n_{e,i} T_{e,i} \tag{2.2}$$

is satisfied. Here, we use the customary shorhand notation $k_B T \to T$. k_B is the Boltzmann's constant. Besides, we have the following Maxwell's equations.

$$\nabla \times \boldsymbol{E} = -\frac{\partial \boldsymbol{B}}{\partial t}, \tag{2.3a}$$

$$\nabla \times \boldsymbol{B} = \mu_0 e (n_i \boldsymbol{u_i} - n_e \boldsymbol{u_e}) + \frac{1}{c^2} \frac{\partial \boldsymbol{E}}{\partial t}, \tag{2.3b}$$

$$\nabla \cdot \boldsymbol{E} = \frac{e}{\epsilon_0} (n_i - n_e), \tag{2.3c}$$

$$\nabla \cdot \boldsymbol{B} = 0. \tag{2.3d}$$

In these equations, the electromagnetic variables are the electric field $\boldsymbol{E}$, the magnetic field $\boldsymbol{B}$ and the current density $\boldsymbol{j}$. This set of equations is not closed. There are more unknowns than equations. We need substantial additional information concerning the variable $\boldsymbol{\pi}_\alpha$, $\boldsymbol{q}_\alpha$, $\boldsymbol{R}$ and Q_α to be able to express them in terms of fluid variables n_α, $\boldsymbol{u}_{\boldsymbol{\alpha}}$, p_α, T_α and electromagnetic fields. Such informatin comes from transport theory ([3]-[5]).

The resultant transport closure relations have a complicated form due to anisotropies induced by the presence of the magnetic field. But these non-ideal terms generated by collisions are neglected compared with the ideal terms. For example, the leading-order effect of the $\boldsymbol{\pi}_i$ have the form:

$$\pi_{i,jj} \sim \mu(2\nabla_\parallel \cdot \boldsymbol{u}_{i,\parallel} - \frac{2}{3}\nabla \cdot \boldsymbol{u}_i) \sim \mu v_{th,i}/L \tag{2.4}$$

where the viscosity coefficeint μ is given by

$$\mu \sim nT_i\tau_i. \tag{2.5}$$

L is the characteristic length of phenomena of interest and $\nabla_\parallel$ stands for the differentiation along the magnetic field lines. If we compare the viscosity term with the ∇p_i term appeared in the momentum equation,

$$|\nabla \cdot \boldsymbol{\pi}_i/\nabla p_i| \sim v_{th,i}\tau_i/L \tag{2.6}$$

is derived. This ratio is typically much smaller than 1 for the sufficiently collisional plasma, so that we can neglect $\boldsymbol{\pi}_i$. In the same way, the terms related to $\boldsymbol{R}$, $\boldsymbol{\pi}_e$, Q_i, Q_e, $\boldsymbol{q}_i$ and $\boldsymbol{q}_e$, can be neglected in collisional plasmas. This peculiear bahavior that terms generated by collisions can be neglected in the sufficiently collisional case can be understood as follows: Due to collisions, anisotropy is reduced. Thus, diagonal parts of moments, such as p_α, dominate non-diagonal parts of moments, that is, we can neglect non-ideal terms.

The model neglecting the non-ideal effects is called ideal two-fluid model.

The forms of equations are as follows:

$$\frac{dn_i}{dt} = -n_i \nabla \cdot \boldsymbol{u}_i, \qquad \frac{dn_e}{dt} = -n_e \nabla \cdot \boldsymbol{u}_e, \tag{2.7a}$$

$$m_i n_i \frac{d\boldsymbol{u}_i}{dt} = e n_i (\boldsymbol{E} + \boldsymbol{u}_i \times \boldsymbol{B}) - \nabla p_i, \tag{2.7b}$$

$$m_e n_e \frac{d\boldsymbol{u}_e}{dt} = -e n_e (\boldsymbol{E} + \boldsymbol{u}_e \times \boldsymbol{B}) - \nabla p_e, \tag{2.7c}$$

$$\frac{dp_i}{dt} = -\gamma p_i \nabla \cdot \boldsymbol{u}_i, \qquad \frac{dp_e}{dt} = -\gamma p_e \nabla \cdot \boldsymbol{u}_e, \tag{2.7d}$$

$$\nabla \times \boldsymbol{E} = -\frac{\partial \boldsymbol{B}}{\partial t}, \qquad \nabla \cdot \boldsymbol{B} = 0, \tag{2.7e}$$

$$\nabla \times \boldsymbol{B} = \mu_0 \boldsymbol{j} + \frac{1}{c^2}\frac{\partial \boldsymbol{E}}{\partial t}, \qquad \nabla \cdot \boldsymbol{E} = \frac{e}{\epsilon_0}(n_i - n_e), \tag{2.7f}$$

where d/dt is the Lagrange differentiation for each species and $\gamma = 5/3$. As we can recognize from the linear dispersion relation of the ideal two-fluid model, this model still contains high-frequency and short-wavelength motions.

Concentrating our interest on the macroscopic and slow fluid motion, we can derive ideal MHD model from the ideal two-fluid model. To achieve it, we introduce appropriate single-fluid variables. The two-fluid equations are rewritten as a set of single-fluid equations.

They are obtained as linear combinations of the pairs of the mass conservation equations for n_e and n_i, and of the momentum conservation equations for $\boldsymbol{u}_e$ and $\boldsymbol{u}_i$, and the sum of the energy conservation equation for p_e and p_i. We define the one-fluid variables as follows:

$$\rho \equiv n_e m_e + n_i m_i \qquad \text{(total mass density)}, \tag{2.8a}$$

$$\tau \equiv e(n_i - n_e) \qquad \text{(charge density)}, \tag{2.8b}$$

$$\rho \boldsymbol{u} \equiv n_e m_e \boldsymbol{u}_e + n_i m_i \boldsymbol{u}_i \qquad \text{(momentum density)}, \tag{2.8c}$$

$$\boldsymbol{j} \equiv e(n_i \boldsymbol{u}_i - n_e \boldsymbol{u}_e) \qquad \text{(current density)}, \tag{2.8d}$$

$$p \equiv p_e + p_i = (n_e + n_i)T \qquad \text{(pressure)}, \tag{2.8e}$$

Inversely, two fluid variables are expressed in terms of one-fluid variables.

$$n_e = \frac{\rho - (m_i/e)\tau}{m_i(1+\mu)} \sim \frac{\rho}{m_i(1+\mu)}, \tag{2.9a}$$

$$n_i = \frac{\rho + \mu(m_i/e)\tau}{m_i(1+\mu)} \sim \frac{\rho}{m_i(1+\mu)}, \tag{2.9b}$$

$$\boldsymbol{u}_e = \frac{\rho\boldsymbol{u} - (m_i/e)\boldsymbol{j}}{\rho - (m_i/e)\tau} \sim \boldsymbol{u} - \frac{m_i}{e}\frac{\boldsymbol{j}}{\rho}, \tag{2.9c}$$

$$\boldsymbol{u}_i = \frac{\rho\boldsymbol{u} + \mu(m_i/e)\boldsymbol{j}}{\rho + \mu(m_i/e)\tau} \sim \boldsymbol{u} + \mu\frac{m_i}{e}\frac{\boldsymbol{j}}{\rho}, \tag{2.9d}$$

$$p_e = \frac{n_e}{n_e + n_i}p \sim \frac{1}{2}p, \tag{2.9e}$$

$$p_i = \frac{n_i}{n_e + n_i}p \sim \frac{1}{2}p. \tag{2.9f}$$

Here, μ is the mass ratio m_e/m_i. The approximations on the RHS are due to the assumption of quasi charge neutrality:

$$|n_i - n_e| \ll n_e. \tag{2.10}$$

This approximation is extremely well satisfied for plasma phenomena with a hydrodynamic (macroscopic) length scale

$$\lambda_H \gg \lambda_D \equiv v_{th,e}/(\sqrt{2}\omega_{pe}). \tag{2.11}$$

The estimation of the ordering is as follows:

$$\begin{aligned}
\frac{|n_i - n_e|}{n_e} &\sim \frac{1}{n_e}\frac{\epsilon_0 E}{m_e\lambda_H}, \\
&= \left(\frac{\epsilon_0 m_e}{n_e e^2}\right)\frac{eE}{m_e\lambda_H}, \\
&\sim \frac{1}{\omega_{pe}^2}\frac{e}{m_e\lambda_H}\frac{m_e v_{th,e}\omega}{e}, \qquad \text{(momentum equation)} \\
&= \frac{\omega^2}{\omega_{pe}^2}, \qquad \text{(assuming } v_{th,e} = \lambda_H\omega \text{)} \\
&= \frac{\lambda_D^2}{\lambda_H^2}.
\end{aligned} \tag{2.12}$$

Further, we can neglect the displacement current, since the order of the flow or the phase velocity of the wave is much smaller than the speed of light in

the macroscopic range. Adding the equation (2.1a) multiplied by m_i and the equation (2.1b) multiplied by m_e gives the equation of mass conservation:

$$\frac{\partial \rho}{\partial t} + \nabla \cdot (\rho \boldsymbol{u}) = 0, \tag{2.13}$$

whereas multiplication by the charges and subtraction results in the equation of charge conservation:

$$\frac{\partial \tau}{\partial t} + \nabla \cdot \boldsymbol{j} = 0. \tag{2.14}$$

Likewise, adding the pair of momentum equations results in the equation of motion:

$$\rho \frac{\partial \boldsymbol{u}}{\partial t} + \rho(\boldsymbol{u} \cdot \nabla)\boldsymbol{u} + \mu \left(\frac{m_i}{e}\right)^2 \nabla \cdot \left(\frac{1}{\rho}\boldsymbol{j}\boldsymbol{j}\right) = -\nabla p + \tau \boldsymbol{E} + \boldsymbol{j} \times \boldsymbol{B}. \tag{2.15}$$

The electron momentum equation multiplied by e/m_e, subtracted from the ion momentum equation multiplied by e/m_i gives the generalized Ohm's law:

$$\begin{aligned} \frac{\partial \boldsymbol{j}}{\partial t} + \nabla \cdot \left[\boldsymbol{j}\boldsymbol{u} + \boldsymbol{u}\boldsymbol{j} - \frac{m_i}{e}(1-\mu)\frac{1}{\rho}\boldsymbol{j}\boldsymbol{j}\right] \\ + \frac{1}{\mu}\frac{e}{m_i}\left[(1-\mu)\boldsymbol{j} \times \boldsymbol{B} - \frac{1-\mu}{2}\nabla p\right] - \\ \frac{1}{\mu}\left(\frac{e}{m_i}\right)^2 \rho(\boldsymbol{E} + \boldsymbol{v} \times \boldsymbol{B}) = 0 \end{aligned} \tag{2.16}$$

Finally, addition of the pressure equation for each species results in the energy equation:

$$\begin{aligned} \frac{\partial p}{\partial t} + (\boldsymbol{u} \cdot \nabla)p + \gamma p(\nabla \cdot \boldsymbol{u}) \\ + \frac{1-\mu}{2}\frac{m_i}{e}\left[(\gamma - 1)\frac{1}{\rho}(\boldsymbol{j} \cdot \nabla)p - \gamma \boldsymbol{j} \cdot \nabla(\frac{p}{\rho})\right] = 0 \end{aligned} \tag{2.17}$$

To consistently derive the large scale dynamics associated with the MHD description, the hydrodynamics length and time scales are chosen to correspond to the size of the plasma:

$$\lambda_{MHD} \equiv |\nabla^{-1}| \sim L \quad \gg r_{L,i} \quad [\gg \lambda_i \gg r_{L,e} \gg \lambda_D] \tag{2.18}$$

$$\tau_{MHD} \equiv |\partial/\partial t|^{-1} \sim L/v_A \quad \gg \Omega_i^{-1} [\gg \omega_{p,i}^{-1} \sim \Omega_e^{-1}] \tag{2.19}$$

The magnitude of the remaining electromagnetic variables are chosen to be set by Ampere's law, Ohm's law, and Poisson's law, respectively:

$$j \sim \frac{B}{\mu_0 L}, \qquad E \sim uB, \qquad \tau \sim \frac{\epsilon_0 E}{L}. \tag{2.20}$$

Let us ged rid of the remaining local two-fluid effects in Eqs. (2.15)-(2.17). First, we consider the momentum equation. The third term in LHS can be compared with another term, for example:

$$\begin{aligned} \frac{|(m_e/m_i)(m_i/e)^2 \nabla \cdot (\boldsymbol{jj}/2)|}{|\boldsymbol{j} \times \boldsymbol{B}|} &\sim \frac{c^2}{\omega_{p,e}^2 L^2} \\ &= \frac{\lambda_e^2}{L^2} \ll 1 \end{aligned} \tag{2.21}$$

The electric field force can be neglected by the quasi-neutral condition. Thus, The momentum equation is reduced to the following form:

$$\rho \frac{\partial \boldsymbol{u}}{\partial t} + \rho(\boldsymbol{u} \cdot \nabla)\boldsymbol{u} = -\nabla p + \boldsymbol{j} \times \boldsymbol{B}. \tag{2.22}$$

Next, we discuss the Ohm's law. Since terms in the first parenthesis is smaller than terms in the second parenthesis, we compare the magnitude of second parenthesis and $\boldsymbol{E}$.

$$\frac{|(m_i/e)(\boldsymbol{j} \times \boldsymbol{B}/\rho)|}{E} \sim \frac{\omega}{\Omega_i} \tag{2.23}$$

Therefore, Ohm's law can be simplified as the following:

$$\boldsymbol{E} + \boldsymbol{u} \times \boldsymbol{B} = 0. \tag{2.24}$$

In the same way, the energy equation can be reduced to the form,

$$\frac{\partial p}{\partial t} + (\boldsymbol{u} \cdot \nabla) = -\gamma p (\nabla \cdot \boldsymbol{u}) \tag{2.25}$$

Here, we summrize ideal MHD equations.

$$\frac{d\rho}{dt} = -\rho\nabla\cdot\boldsymbol{u}, \tag{2.26a}$$

$$\rho\frac{d\boldsymbol{u}}{dt} = -\nabla p + \boldsymbol{j}\times\boldsymbol{B}, \tag{2.26b}$$

$$\frac{dp}{dt} = -\gamma p\nabla\cdot\boldsymbol{u}, \tag{2.26c}$$

$$\frac{\partial\boldsymbol{B}}{\partial t} + \nabla\times\boldsymbol{E} = 0, \tag{2.26d}$$

$$\boldsymbol{E} + \boldsymbol{u}\times\boldsymbol{B} = 0, \tag{2.26e}$$

$$\nabla\times\boldsymbol{B} = \mu_0\boldsymbol{j}, \tag{2.26f}$$

$$\nabla\cdot\boldsymbol{B} = 0. \tag{2.26g}$$

Because of its simplicity, this model is frequently analized in plasma physics.

2.2 Conventional variational principle of MHD

Most of laws of nature can be formulated in terms of minimization or extremal principles, which expresses the idea that laws of nature should come from setting a derivative of some quantity, the action, to be zero. Variational principles provide a framework for Twentieth Century physics: the most successful models of physics, Maxwell's equations, Schrödinger's equation, etc., all have variational principle (Lagrange formulation) and associated Hamiltonian formulation. The same is true for the most important models of plasma physics, such as MHD, as we will show later.

In general, the formulation by variational principle has practical reasons, for example, we can provide conservation laws in terms of Lagrangian's symmetry. Besides, since the Lagrangian has a form independent of a coordinate, we can easily derive a basic equation for a general, non-inertial, coordinate. Lagrange formulation for MHD or, more directly, variational priciple for the Hamiltonian of MHD is useful to analyze stability of a system. Such analysis is called energy principle.

Here, I mention the variational principle for MHD, which was established many years ago. The equation of motion of MHD is derived by variation of the Lagrangian:

$$L_{MHD} = \int(\frac{1}{2}\rho u^2 - \rho\epsilon - \frac{1}{2}B^2)dx^3 \tag{2.27}$$

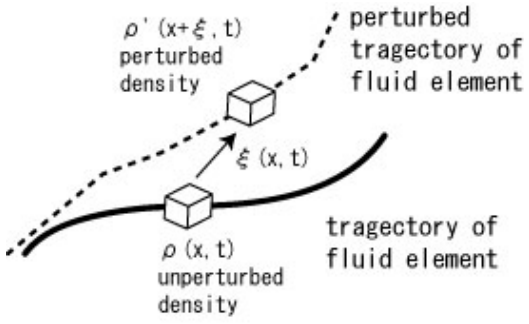

Figure 2.1: Schematic picture of variation.

where, ρ is the mass density, ϵ is the internal energy and $\boldsymbol{u}$ is the flow of the MHD fluid. As you see, degrees of freedom is infinite. Variational principle for systems having infinite degrees of freedom is somewhat problematic: in the variational principle of fluid dynamics, having a Lagrangian simpler than MHD, Eulerian form of variation with Lagrange multipliers give inadequate potential desciption of velocity field ([18], [32-35]).

Thus we employ a variation based on the Lagrange description of motion. A Lagrange description of fluid motion is based on the positions of fluid elements as a function of time. Let $\boldsymbol{x}(\boldsymbol{a}, t)$, the position of a fluid element, be a function of initial position $\boldsymbol{a}$ and time t. Thus $\boldsymbol{x}(\boldsymbol{a}, 0) = \boldsymbol{a}$. The inverse function of $\boldsymbol{x}(\boldsymbol{a}, t)$ is defined as $\boldsymbol{a} = \boldsymbol{x}^{-1}(\boldsymbol{x}, t)$. The Eulerian fluid velocity at the point $\boldsymbol{x}$, is related with Lagrangian fluid velocity as

$$\boldsymbol{u}(\boldsymbol{x}, t) = \left.\frac{\partial \boldsymbol{x}(\boldsymbol{a}, t)}{\partial t}\right|_{\boldsymbol{a}=\boldsymbol{x}^{-1}(\boldsymbol{x},t)} = \frac{D\boldsymbol{x}}{Dt}. \tag{2.28}$$

Consider a displacement vector $\boldsymbol{\xi}(\boldsymbol{x}, t)$, that is,

$$\boldsymbol{x}(\boldsymbol{a}, t) \to \boldsymbol{x}(\boldsymbol{a}, t) + \boldsymbol{\xi}(\boldsymbol{x}, t). \tag{2.29}$$

Due to the displacement, physical variables appearing in the Lagrangian are modified, that is, $A(\boldsymbol{x}, t) \to A'(\boldsymbol{x}, t) = A(\boldsymbol{x}, t) + \delta A(\boldsymbol{x}, t)$. We can relate the displacement vector $\boldsymbol{\xi}$ and variation of variables $\rho, \epsilon, \boldsymbol{u}$ and $\boldsymbol{B}$ in terms of conservation laws which MHD fluid must satisfy, that is, we impose some restrictions to variables. For example, the variation of the mass density is

estimated by mass conservation law. Mass of a fluid element is conserved in the perturbation. If we denote Δ as a variation along the displacement,

$$\begin{aligned} \Delta(\rho dx^3) &= (\Delta\rho)dx^3 + \rho(\Delta dx^3) = 0, \\ &= (\Delta\rho + \rho(\nabla\cdot\boldsymbol{\xi}))dx^3 = 0, \\ \rightarrow \quad \Delta\rho &= -\rho(\nabla\cdot\boldsymbol{\xi}), \end{aligned} \tag{2.30}$$

here we used $\Delta dx^3 = (\nabla\cdot\boldsymbol{\xi})dx^3$. This $\Delta\rho$ denotes $\rho'(\boldsymbol{x}+\boldsymbol{\xi}) - \rho(\boldsymbol{x})$, thus $\delta\rho$ is given by

$$\delta\rho(\boldsymbol{x},t) = \Delta\rho - (\boldsymbol{\xi}\cdot\nabla)\rho = -\nabla\cdot(\rho\boldsymbol{\xi}). \tag{2.31}$$

Using $\delta\rho$, variation of the internal energy $\delta\epsilon$ is given as

$$\delta\epsilon = \frac{\partial\epsilon}{\partial\rho}\delta\rho = \frac{p}{\rho^2}\delta\rho. \tag{2.32}$$

In the same way, $\delta\boldsymbol{B}$ is given by

$$\delta\boldsymbol{B} = \nabla\times(\boldsymbol{\xi}\times\boldsymbol{B}) \tag{2.33}$$

in terms of magnetic flux conservation. This is obtained by the induction equation,

$$\frac{\partial\boldsymbol{B}}{\partial t} = \nabla\times(\boldsymbol{u}\times\boldsymbol{B}). \tag{2.34}$$

The variation of the velocity field can be estimated as follows: the velocity field of the perturbed state $\boldsymbol{u}'$ is given by

$$\boldsymbol{u}'(\boldsymbol{x}+\boldsymbol{\xi},t) = \frac{D(\boldsymbol{x}+\boldsymbol{\xi})}{Dt} = \boldsymbol{u}(\boldsymbol{x},t) + \frac{\partial\boldsymbol{\xi}}{\partial t} + (\boldsymbol{u}\cdot\nabla)\boldsymbol{\xi}, \tag{2.35}$$

where Lagrange derivative $D\boldsymbol{\xi}/Dt = (\partial\boldsymbol{\xi}/\partial t) + (\boldsymbol{u}\cdot\nabla)\boldsymbol{\xi}$. Thus, $\delta\boldsymbol{u}(\boldsymbol{x},t) = \boldsymbol{u}' - \boldsymbol{u}$ is given by

$$\delta\boldsymbol{u}(\boldsymbol{x},t) = \frac{\partial\boldsymbol{\xi}}{\partial t} + (\boldsymbol{u}\cdot\nabla)\boldsymbol{\xi} - (\boldsymbol{\xi}\cdot\nabla)\boldsymbol{u}. \tag{2.36}$$

Eventually, variation of variables by the displacement $\boldsymbol{\xi}$, are as follows:

$$\delta\boldsymbol{u} = \frac{\partial\boldsymbol{\xi}}{\partial t} + (\boldsymbol{u}\cdot\nabla)\boldsymbol{\xi} - (\boldsymbol{\xi}\cdot\nabla)\boldsymbol{u}, \tag{2.37a}$$

$$\delta\rho = -\nabla\cdot(\rho\boldsymbol{\xi}), \tag{2.37b}$$

$$\delta\epsilon = \frac{p}{\rho^2}\delta\rho, \tag{2.37c}$$

$$\delta\boldsymbol{B} = \nabla\times(\boldsymbol{\xi}\times\boldsymbol{B}). \tag{2.37d}$$

Consider a variation of the action,

$$\delta I = \int dt L_{MHD}, \tag{2.38}$$

we derive a equation of motion, that is,

$$\rho \frac{\partial \boldsymbol{u}}{\partial t} + (\boldsymbol{u} \cdot \nabla)\boldsymbol{u} = -\nabla p + \boldsymbol{j} \times \boldsymbol{B}. \tag{2.39}$$

The details of calculation is shown in Appendix A.1.

Here we discuss the variational principle in terms of L_{MHD}. The Lagrangian L_{MHD} contains the potential energy $B^2/2$. This term does not appear in the Lagrangian for a charged particle, since the magnetic field has no ability to exchange energy with the particle. Therefore, the lagrangian L_{MHD} is based on the idea that a plasma can be understood as macroscopic fluid flow intercting with electromagnetic fields. However, since a plasma is constituted by charged particles so that we may construct a variational principle, which takes into account the particle view. In the next section, I will derive a equation of motion for MHD model by a variational principle using a two-fluid Lagrangian extended from the particle's Lagrangian.

2.3 Relation between variational principle for MHD and for two-fluid model

2.3.1 Variational principle for single-fluid plasma

Before proceeding to discuss the relation between variational principles for two-fluid and MHD models, here I introduce a variational principle for single fluid plasma. The Lagrangian for a charged particle is defined as:

$$L_{par} = \int \frac{1}{2} m \dot{\boldsymbol{x}}^2 + e\dot{\boldsymbol{x}} \cdot \boldsymbol{A} - e\phi. \tag{2.40}$$

where, $\boldsymbol{A}$ is the magnetic vector potential, ϕ is the electrostatic potential, $\dot{\boldsymbol{x}}$ is the velocity and m is the mass of a particle. Extending the particle's Lagrangian, we can construct a Lagrangian for a charged fluid. For example, about an ion fluid, the lagrangian L_i is given as:

$$L_i = \int dx^3 (\frac{1}{2}\rho_i u_i^2 - \rho_i \epsilon_i + e n_i \boldsymbol{u}_i \cdot \boldsymbol{A} - e n_i \phi), \tag{2.41}$$

where n_i is the number density, and $\rho_i = m_i n_i$ is the mass density of the ion fluid. We consider a displacement $\boldsymbol{\xi}_i$ as with the last section. Although, in the conventional Lagrange formulation of MHD, we estimate the variation in terms of mass conservation and magnetic flux conservation, Here, variation of variables induced by the displacement $\boldsymbol{\xi}_i$ are evaluated as follows:

$$\delta n_i = -\nabla \cdot (n_i \boldsymbol{\xi}_i) \qquad \text{(conservation of number of particles)}, \tag{2.42a}$$

$$\delta \rho_i = -\nabla \cdot (\rho_i \boldsymbol{\xi}_i), \qquad \text{(mass conservation)} \tag{2.42b}$$

$$\delta \boldsymbol{u}_i = \frac{\partial \boldsymbol{\xi}_i}{\partial t} + (\boldsymbol{u}_i \cdot \nabla)\boldsymbol{\xi}_i - (\boldsymbol{\xi}_i \cdot \nabla)\boldsymbol{u}_i, \tag{2.42c}$$

$$\delta \epsilon_i = \frac{\partial \epsilon_i}{\partial \rho_i}\delta\rho_i = \frac{p_i}{\rho_i^2}\delta\rho_i, \tag{2.42d}$$

$$\delta \boldsymbol{A} = 0, \qquad \delta\phi = 0. \tag{2.42e}$$

Here, I assumed that the displacement does not affect the electromagnetic field. This assumption, also employed in the variational principle for the charged particle, means that vatiation with respect to $\boldsymbol{\xi}_i$ and $\boldsymbol{A}$ can be treated independently. Thus, variation of the action can be estimated in terms of equation (2.42) as,

$$\delta I = \delta \int dt dx^3 \left\{ \frac{1}{2}\rho_i u_i^2 - \rho_i \epsilon_i + e n_i \boldsymbol{u}_i \cdot \boldsymbol{A} - e n_i \phi \right\} \tag{2.43}$$

$$= \int dt dx^3 \{ \frac{u^2}{2}\delta\rho_i + \rho_i \boldsymbol{u}_i \cdot \delta \boldsymbol{u}_i - \delta\rho_i \epsilon_i - \rho_i \delta\epsilon_i + e\delta n_i \boldsymbol{u}_i \cdot \boldsymbol{A} + e n_i \delta \boldsymbol{u}_i \cdot \boldsymbol{A} + e n_i \boldsymbol{u}_i \cdot \delta \boldsymbol{A} - e\delta n_i \phi - e n_i \delta\phi \} \tag{2.44}$$

$$= \int dt dx^3 \{ -\frac{u_i^2}{2}\nabla\cdot(\rho_i\boldsymbol{\xi}_i) + \boldsymbol{u}_i \cdot \big(\frac{\partial \boldsymbol{\xi}_i}{\partial t} + (\boldsymbol{u}_i\cdot\nabla)\boldsymbol{\xi}_i - (\boldsymbol{\xi}_i\cdot\nabla)\boldsymbol{u}_i\big) - e(\boldsymbol{u}_i\cdot\boldsymbol{A})\nabla\cdot(n_i\boldsymbol{\xi}_i) + e n_i \boldsymbol{A}\cdot\big(\frac{\partial \boldsymbol{\xi}_i}{\partial t} + (\boldsymbol{u}_i\cdot\nabla)\boldsymbol{\xi}_i - (\boldsymbol{\xi}_i\cdot\nabla)\boldsymbol{u}_i\big) + e\phi\nabla\cdot(n_i\boldsymbol{\xi}_i) + \epsilon_i\nabla\cdot(\rho_i\boldsymbol{\xi}_i) + \frac{p_i}{\rho_i}\nabla\cdot(\rho_i\boldsymbol{\xi}) \}. \tag{2.45}$$

We integrate all terms by parts and drop surface integrals by boundary conditions, such as $\boldsymbol{\xi}_i(|\boldsymbol{x}| \to \infty) = 0$ and $\boldsymbol{\xi}_i(\boldsymbol{x}, t_1) = \boldsymbol{\xi}_i(\boldsymbol{x}, t_2) = 0$ (for any $\boldsymbol{x}$). After the calculation, δI can be written as:

$$\delta I = \int dt dx^3 \boldsymbol{\xi}_i \cdot \left\{ -\rho_i \frac{\partial \boldsymbol{u_i}}{\partial t} - \rho_i (\boldsymbol{u}_i \cdot \nabla)\boldsymbol{u}_i + e n_i (-\frac{\partial \boldsymbol{A}}{\partial t} - \nabla\phi) - \nabla p_i + e n_i (\boldsymbol{u}_i \times \boldsymbol{B}) \right\}. \tag{2.46}$$

The details of the calculation is shown in Appendix A.2. Setting δI to be zero, we derive a equation of motion for the ion fluid as

$$\rho_i \frac{d\boldsymbol{u}_i}{dt} = en_i(\boldsymbol{E} + \boldsymbol{u}_i \times \boldsymbol{B}) - \nabla p_i. \tag{2.47}$$

We summarize the discussion above. We can derive the fluid momentum equation by a variational principle based on the Lagrangian, extending the particle's one, using the mass conservation law. That is, one species fluid plasma still keep the characteristic of the particle within the framework of variational principle.

2.3.2 Variational principle for two-fluid model

Next, we consider a variational principle for two-fluid plasma. In this case, we should take our Lagrangian as,

$$L_{two} = L_i + L_e + L_{EM}, \tag{2.48}$$

where L_i is the Lagrangian for the ion plasma, L_e is the Lagrangian for the electron plasma and L_{EM} is the Lagrangian for the electromagnetic field. The reason why I included the electromagnetic part is to provide a closed set of equations of two-fluid model. Concrete form of the Lagrangian is given as

$$\begin{aligned} L_{two} = \int dx^3 \{ \frac{\rho_i}{2} u_i^2 + \frac{\rho_e}{2} u_e^2 - \rho_i \epsilon_i - \rho_e \epsilon_e + e(n_i \boldsymbol{u}_i - n_e \boldsymbol{u}_e) \cdot \boldsymbol{A} \\ - e(n_i - n_e)\phi + \frac{\epsilon_0}{2}(-\nabla\phi - \frac{\partial \boldsymbol{A}}{\partial t})^2 - \frac{1}{2\mu_0}(\nabla \times \boldsymbol{A})^2 \} \end{aligned} \tag{2.49}$$

At this stage, we know the form of $\boldsymbol{B}$ and $\boldsymbol{E}$ expressed by potentials,

$$\boldsymbol{E} = -\nabla\phi - \frac{\partial \boldsymbol{A}}{\partial t}, \qquad \boldsymbol{B} = \nabla \times \boldsymbol{A}. \tag{2.50}$$

From these equations, we can obtain two Maxwell's equations. They are given as:

$$\frac{\partial \boldsymbol{B}}{\partial t} = -\nabla \times \boldsymbol{E}, \qquad \nabla \cdot \boldsymbol{B} = 0. \tag{2.51}$$

Besides, when we take a variation with respect to a displacement $\boldsymbol{\xi}$, we use the mass conservation law of each fluid. We already have the continuity equation:

$$\frac{dn_\alpha}{dt} = -n_\alpha \nabla \cdot \boldsymbol{u}_\alpha \tag{2.52}$$

From these information, we derive rest of equations of the two-fluid model, that is, the equations of motion and two Maxwell's equations. The Maxwell's equations are derived from the variation with respecto to ϕ and $\boldsymbol{A}$. At first, we consider a variation with respect to ϕ.

$$\delta I = \int dtdx^3 \left\{ -e(n_i - n_e)\delta\phi + \epsilon_0(-\nabla\phi - \frac{\partial \boldsymbol{A}}{\partial t})(-\nabla\delta\phi) \right\} \tag{2.53}$$

Integragion of the second term by parts and dropping the surface integrals, give

$$\delta I = \int dtdx^3 \left\{ \delta\phi(-e(n_i - n_e) + \epsilon_0 \nabla \cdot \boldsymbol{E}) \right\} \tag{2.54}$$

Setting δI to be zero, we derive the Poisson's equation,

$$\nabla \cdot \boldsymbol{E} = \frac{e}{\epsilon_0}(n_i - n_e) \tag{2.55}$$

Next, we consider a variation with respect to $\boldsymbol{A}$. In that case,

$$\begin{aligned} \delta I = \int dtdx^3 \{\ & e(n_i \boldsymbol{u}_i - n_e \boldsymbol{u}_e) \cdot \delta \boldsymbol{A} \\ & + \epsilon_0(-\nabla\phi - \frac{\partial \boldsymbol{A}}{\partial t})(-\delta\frac{\partial \boldsymbol{A}}{\partial t}) - \delta\big(\frac{1}{2\mu_0}(\nabla \times \boldsymbol{A})^2\big)\ \}. \end{aligned} \tag{2.56}$$

The last term of eq.(2.56) can be written as

$$\delta\big(\frac{1}{2\mu_0}(\nabla \times \boldsymbol{A})^2\big) = \delta\big(\frac{1}{2\mu_0}\epsilon^{ijk}\frac{\partial A^k}{\partial x^j}\epsilon^{ilm}\frac{\partial A^m}{\partial x^l}\big) \tag{2.57}$$

$$= \delta\big(\frac{1}{2\mu_0}(\delta^{jl}\delta^{km} - \delta^{jm}\delta^{kl})\frac{\partial A^k}{\partial x^j}\frac{\partial A^m}{\partial x^l}\big) \tag{2.58}$$

$$= \frac{1}{\mu_0}\big(\frac{\partial A^k}{\partial x^j}\frac{\partial \delta A^k}{\partial x^j} - \frac{\partial \delta A^k}{\partial x^j}\frac{\partial A^j}{\partial x^k}\big) \tag{2.59}$$

$$= \delta\boldsymbol{A} \cdot \big(-\frac{1}{\mu_0}\nabla^2\boldsymbol{A} + \frac{1}{\mu_0}\nabla(\nabla \cdot \boldsymbol{A})\big) \tag{2.60}$$

$$= \delta\boldsymbol{A} \cdot \big(\frac{1}{\mu_0}\nabla \times (\nabla \times \boldsymbol{A})\big), \tag{2.61}$$

where ϵ^{ijk} is the Levi-Civita symbol which is the three-dimensional tensor defined as totally antisymmetric in all three indices. Besides, δ^{ij} is the Kronecker's delta defined as

$$\delta^{jk} = 1 \quad \text{for} \quad j = k, \tag{2.62}$$

$$\delta^{jk} = 0 \quad \text{for} \quad j \neq k. \tag{2.63}$$

We use the vector identity,

$$\nabla \times (\nabla \times \boldsymbol{A}) = \nabla(\nabla \cdot \boldsymbol{A}) - \nabla^2 \boldsymbol{A}. \tag{2.64}$$

Therefore, eq. (2.56) is written as

$$\delta I = \int dt dx^3 \{\delta \boldsymbol{A} \cdot \left(e(n_i \boldsymbol{u}_i - n_e \boldsymbol{u}_e) + \epsilon_0 \frac{\partial \boldsymbol{E}}{\partial t} - \frac{1}{\mu_0} \nabla \times \boldsymbol{B} \right)\}. \tag{2.65}$$

Thus, if we set δI to be zero, we derive the Maxwell's equation,

$$\nabla \times \boldsymbol{B} = \mu_0 \boldsymbol{j} + \frac{1}{c^2} \frac{\partial \boldsymbol{E}}{\partial t}. \tag{2.66}$$

At last, taking variation with respect to the displacement of each fluid, $\boldsymbol{\xi}_i$ and $\boldsymbol{\xi}_e$, as in the single fluid plasma, we derive a equation of motion for each species,

$$\rho_i \frac{d\boldsymbol{u}_i}{dt} = e n_i (\boldsymbol{E} + \boldsymbol{u}_i \times \boldsymbol{B}) - \nabla p_i, \tag{2.67}$$

$$\rho_e \frac{d\boldsymbol{u}_e}{dt} = -e n_e (\boldsymbol{E} + \boldsymbol{u}_e \times \boldsymbol{B}) - \nabla p_e. \tag{2.68}$$

Here we assumed that the displacements $\boldsymbol{\xi}_e$ and $\boldsymbol{\xi}_i$ generate no variation of electromagnetic fields, since we regarded vatiations with respect to $\boldsymbol{\xi}_{i,e}$, $\boldsymbol{A}$ and ϕ as independent.

We summarize the discussion in this section. Starting from the Lagrangian L_{two} with the continuity equations and two of Maxwell's equations, we derive the rest of Maxwell equations and equation of motion for each fluid.

2.3.3 MHD equation of motion derived from two-fluid Lagrangian

In the previous section 2.1, the equation of motion of MHD is derived by the linear combination of equation of motion of electron's and ion's, with the quasi-neutral condition. Here, performing a manipulation having the same meaning of linear combination in a context of variational principle, we derive a equation of motion of MHD in terms of the two-fluid Lagrangian. At first, we write the two-fluid Lagrangian in terms of single-fluid variables as

$$L = \int dt^2 \left[\frac{\rho}{2} u^2 + \boldsymbol{A} \cdot \boldsymbol{j} - \rho \epsilon \right] \tag{2.69}$$

where $\rho_i \sim \rho$, $\boldsymbol{u}_i \sim \boldsymbol{u}$ and $\rho_i\epsilon_i \sim \rho\epsilon$, because of the small electron mass, and the electrostatic potential term disappears due to the charge neutral condition. The electromagnetic part of the Lagrangian L_{EM} is not concerned since it does not affect the momentum equation as far as we regard variations with respect to electromagnetic fields and the fluid displacement as independent. We will consider a variation using the Lagrangian shown in eq. (2.69),

$$\delta I = \int dtdx^3[\frac{u^2}{2}\delta\rho + \rho\boldsymbol{u}\cdot\delta\boldsymbol{u} + \delta\boldsymbol{A}\cdot\boldsymbol{j} + \boldsymbol{A}\cdot\delta\boldsymbol{j} - \delta\rho\epsilon - \rho\frac{\partial\epsilon}{\partial\rho}\delta\rho]. \quad (2.70)$$

Variation of variables can be expressed in terms of the ion displacement $\boldsymbol{\xi}$ as follows:

$$\delta\rho = -\nabla\cdot(\rho\boldsymbol{\xi}), \quad (2.71)$$

$$\delta A = 0, \quad (2.72)$$

$$\delta\boldsymbol{u} = \frac{\partial\boldsymbol{\xi}}{\partial t} + (\boldsymbol{u}\cdot\nabla)\boldsymbol{\xi} - (\boldsymbol{\xi}\cdot\nabla)\boldsymbol{u}. \quad (2.73)$$

The variation of the current density $\delta\boldsymbol{j}$ is noticed carefully. Our Lagrangian is based on the particles' point of view, that is, the Lagrangian is an extention of the particle's Lagrangian. Therefore we recognize the current density as $\boldsymbol{j} = en(\boldsymbol{u}_i - \boldsymbol{u}_e)$ not $\boldsymbol{j} = \mu_0^{-1}\nabla\times\boldsymbol{B}$, although the latter is employed in the conventional variational principle for MHD. Thus,

$$\begin{aligned}
\delta\boldsymbol{j} &= en(\delta\boldsymbol{u}_i - \delta\boldsymbol{u}_e + e(\boldsymbol{u}_i - \boldsymbol{u}_e)\delta n) \\
&= en\left[\frac{\partial\boldsymbol{\xi}}{\partial t} + (\boldsymbol{u}_i\cdot\nabla)\boldsymbol{\xi} - (\boldsymbol{\xi}\cdot\nabla)\boldsymbol{u}_i - \frac{\partial\boldsymbol{\xi}}{\partial t} - (\boldsymbol{u}_e\cdot\nabla)\boldsymbol{\xi} - (\boldsymbol{\xi}\cdot\nabla)\boldsymbol{u}_e\right] \\
&= (\boldsymbol{j}\cdot\nabla)\boldsymbol{\xi} - n(\boldsymbol{\xi}\cdot\nabla)\frac{\boldsymbol{j}}{n} - \frac{\boldsymbol{j}}{n}\nabla\cdot(n\boldsymbol{\xi}) \\
&= \nabla\times(\boldsymbol{\xi}\times\boldsymbol{j}), \quad (2.74)
\end{aligned}$$

where we assumed that we identified the ion displacement $\boldsymbol{\xi}$ as the electron displacement $\boldsymbol{\xi}_e$, i.e. $\boldsymbol{\xi} = \boldsymbol{\xi}_e$. This manipulation in the variational principle corresponds to the linear comibination of equations in the derivation of MHD momentum equation.

Accomplishing the variation based on the above considerations,

$$\begin{aligned}
\delta I = \int dtdx^3\,[\, &-\frac{u^2}{2}\nabla\cdot(\rho\boldsymbol{\xi}) + \rho\boldsymbol{u}\cdot(\frac{\partial\boldsymbol{\xi}}{\partial t} + (\boldsymbol{u}\cdot\nabla)\boldsymbol{\xi} - (\boldsymbol{\xi}\cdot\nabla)\boldsymbol{u}) \\
&+ \boldsymbol{A}\cdot\nabla\times(\boldsymbol{\xi}\times\boldsymbol{j}) + (\epsilon + \rho\frac{\partial\epsilon}{\partial\rho})\nabla\cdot(\rho\boldsymbol{\xi})\,] \quad (2.75)
\end{aligned}$$

After tedious calculation (details of calculation is shown in Appendix A.3), we obtain the equation of motion for MHD model as

$$\rho(\frac{\partial \boldsymbol{u}}{\partial t} + (\boldsymbol{u} \cdot \nabla)\boldsymbol{u}) = \boldsymbol{j} \times \boldsymbol{B} - \nabla p. \tag{2.76}$$

We summarize the result of this section. We starting from the Lagrangian (2.69) which uses sinle-fluid variables. Considering a displacement of a fluid $\boldsymbol{\xi}$ with variations as

$$\delta\rho = -\nabla \cdot (\rho\boldsymbol{\xi}), \tag{2.77}$$

$$\delta A = 0, \tag{2.78}$$

$$\delta\boldsymbol{u} = \frac{\partial \boldsymbol{\xi}}{\partial t} + (\boldsymbol{u} \cdot \nabla)\boldsymbol{\xi} - (\boldsymbol{\xi} \cdot \nabla)\boldsymbol{u} \tag{2.79}$$

$$\delta\boldsymbol{j} = \nabla \times (\boldsymbol{\xi} \times \boldsymbol{j}), \tag{2.80}$$

we derive the MHD momentum equation. The manipulation that we identify the ion displacement as the electron displacement represents the linear combinations of momentum equations performed in the algebraic derivation of MHD equations. Since the Lagrangian (2.69) is constructed from the particles' view, Lagrangian description (particles' view) is essential to relate MHD model with two-fluid model in the theory of variational principle.

Chapter 3

Smoothed particle hydrodynamics for Hall-MHD

As discussed in Chap. 2, the two-fluid model containing microscopic effects and the macroscopic MHD model can be related by the variational principle based on the Lagrangian constructed by the Lagrangian (particles') view. We consider that a multiscale simulation analyzing micro- and macroscales holistically can be realized in terms of Lagrangian view as in the variational principle. Translating it in a terminology of numerical simulation, the multiscale simulation may be developed in terms of particle method. Contiuous fields of physical variables characterising each stage of the scale hierarchy is considered as a collection of quasi-particles. The discretized quasi-particles move in a computational domain with changing their character depending on the scale they occupy. We call this multiscale algorithm as multiscale (quasi-)particle simulation.

Although there is a wide variety of particle methods, we consider that a set of model equations in each stage of the hierarchy should be discretized in terms of a particle method which integrates in time along the quasi-particle's velocity. In that particle method, $\boldsymbol{v}$ constructs the characteristic curves. In the multiscale particle simulation in terms of the velocity characteristic method, the velocity $\boldsymbol{v}$ is an idea penetrating from micro- to macro-scales in the multiscale simulation.

Particularly, in the fluid model of plasmas, we employ an idea of Smoothed Particle Hydrodynamics (SPH), a particle method simulating neutral fluids, as a discretizing method. The reason for using SPH is as follows: a set of SPH

equations is derived from variational principle about a Lagrangian L_{SPH}, discretized form of the fluid Lagrangian, thus, SPH seems to be deeply related to the principles of dynamics and discussions in Chap. 2. Besides, since application of SPH for MHD has been already developed, we can consider the multiscale quasi-particle method just to develop a particle scheme in the microscopic regime. In this chapter, we aim at a development of SPH for Hall-MHD, the model neglecting the electron-mass in the two-fluid model. Hall-MHD lies just below the macroscopic MHD model in the hierarchy of model equations. Therefore, connection between SPH for Hall-MHD and SPH for MHD (typically called SPMHD) is a starting point of a sequential scale coupling.

At first, we introduce the framework and discipline of SPH.

3.1 Smoothed Particle Hydrodynamics

The standard approach to solve the equations of fluid dynamics numerically is to define fluid quantities on regular spatial grids, computing derivatives using finite difference, finite volume or finite element method. However, for astrophysical fluids, problems frequently involve changes of physical variables in spatial and temporal scales over many orders of magnitude. Typically, we do not need a high resolution in a low density region, while we want to solve carefully in a high density region. Thus, adaptivity, effective distribution of grids, is an essential ingredient which is absent from a fixed-grid approach. Progress in this area has been rapid in recent years with the development of procedures for adaptive mesh refinement (AMR). However, a further constraint is that astrophysical problems are frequently asymmetric. Complicated structure of fields cause numerical diffusion in terms of (fixed or adaptive) Cartesian grids. Other approaches to this problem are to use unstructured grids (where typically the grid is reconstructed at each new time step) or Lagrangian grid methods, where the grid shape deforms according to the flow pattern.

An alternative to all of these methods is to remove the spatial grid entirely, resulting in methods which are inherently adaptive. In this approach, fluid quantities are carried by a set of moving interpolation points, referred to as quasi-paritcles. Derivatives are evaluated either by interpolation in terms

of neighbouring paritcles, or via a hybrid approach by interpolation using overlaid grids as the particle-in-cell (PIC) method.

Smoothed Particle Hydrodyanamics (SPH) is a particle method invented to simulate nonaxisymmetric phenomena in astrophysics (Lucy [36], Gingold & Monaghan [37]).

The advantages of SPH against standard grid based approaches can be summarised as follows: First, SPH is conceptually both simple and beautiful. All of the equations can be derived self-consistently from physical principles with a few basic assumptions. Therefore, a development of numerical algorithm is easier than other methods. Secondly, adaptivity is a built-in feature. The Lagrangian nature of the method means that changes in density and flow are automatically accounted for without the need for mesh refinement or other complicated procedures. As a result of its adaptivity, SPH can distribute numerical efforts efficiently. In a high density region where high resolusion is needed, particles gather together and we can simulate a fine structure automatically. Thirdly, free boundaries, common in astrophysical problems, are simple and natural in SPH. Fourth, a significant advantage in an astrophysical contest is that SPH couples naturally with calculation of self-gravity.

SPH also has a number of disadvantages when compared to finite difference schemes. The first of these is that, SPH involves the additional computational cost of constructing the neighbour lists, algorithm for searching interacting particles. Secondly, SPH suffers from a lack of development of a high speed algorithm. Althogh dependence on problems prevents general evaluation, SPH has a tendency to require computational time longer than finite difference schemes.

The basic of the SPH approach is given as follows. We begin with the identity

$$A(\boldsymbol{x}) = \int A(\boldsymbol{x}')\delta(|\boldsymbol{x} - \boldsymbol{x}'|), \tag{3.1}$$

where A is any variable defined on the spatial coordinate $\boldsymbol{x}$ and δ means the Dirac delta function. This integral is approximated by replacing the delta function with a smoothing kernel W with a characteristic width h, such that

$$\lim_{h\to 0} W(\boldsymbol{x} - \boldsymbol{x}', h) = \delta(\boldsymbol{x} - \boldsymbol{x}'), \tag{3.2}$$

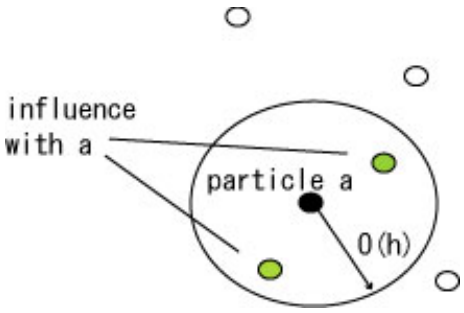

Figure 3.1: Schematic view of SPH compact support

giving

$$A(\boldsymbol{x}) = \int A(\boldsymbol{x}')W(|\boldsymbol{x}-\boldsymbol{x}'|,h)d\boldsymbol{x}' + O(h^2), \tag{3.3}$$

where the term, of the order of $O(h)$, is vanished by the symmetry of the kernel function. The kernel function is normalised as

$$\int W(\boldsymbol{x}-\boldsymbol{x}')d\boldsymbol{x}' = 1. \tag{3.4}$$

Finally the integral (3.3) is discretised onto a finite set of interpolation points (the quasi-particles or just particles) by replacing the integral by a summation and the mass element ρd^3x with the quasi-particle mass m, i.e.,

$$A(\boldsymbol{x}) = \int \frac{A(\boldsymbol{x}')}{\rho(\boldsymbol{x}')}W(|\boldsymbol{x}-\boldsymbol{x}'|,h)\rho(\boldsymbol{x}')d\boldsymbol{x}' + O(h^2) \tag{3.5}$$

$$\approx \sum_{b=1}^{N} m_b \frac{A_b}{\rho_b}W(|\boldsymbol{x}-\boldsymbol{x}_b|,h), \tag{3.6}$$

where the subscipt b refers to the quantity evaluated at the position of particle b. This summation interpolantion is the basis of all SPH formalisms.

We can obtain a derivative of a field function in terms of particles's value and a differentiable kernel W, based on eq. (3.6). Derivatives of this interpolant can be obtained by ordinary differentiation; there is no need to use finite differences and no need for grids. For example, if we want to evaluate ∇A, it is given as

$$\nabla A(\boldsymbol{x}) = \sum_b m_b \frac{A_b}{\rho_b}\nabla W(|\boldsymbol{x}-\boldsymbol{x}_b|,h). \tag{3.7}$$

For gradient about a paricle a at $\boldsymbol{x}_a$,

$$\nabla A_a = \sum_b m_b \frac{A_b}{\rho_b} \nabla W_{ab} \tag{3.8}$$

where $\nabla_{ab} \equiv \nabla W(\boldsymbol{x} - \boldsymbol{x}_b, h)|_{\boldsymbol{x}=\boldsymbol{x}_a}$. Likewise, to obtain higher accuracy, we would obtain other interpolant for the gradient, it is given by

$$\begin{aligned} \nabla A &= \frac{1}{\rho}[A\nabla\rho - \nabla(\rho A)], & (3.9) \\ &\approx \frac{1}{\rho_a} \sum_b m_b (A_b - A_a) \nabla_a W_{ab}. & (3.10) \end{aligned}$$

Although the summation are formally over all the particles, only a small number actually contribute because W can be chosen so that it falls rapidly at $|\boldsymbol{x} - \boldsymbol{x}_b| \geq h$ (compact support discussed below). This neglection of contributions by distant particles improves the efficiency of SPH.

We can choose any smoothing kernel W as long as it satisfies some properties. All the major properites are summarized below.

1. The smoothing kernel must be normalized.

2. The smoothing kernel should be compactly supported, i.e.,

$$W(\boldsymbol{x} - \boldsymbol{x}') = 0, \quad \text{for } |\boldsymbol{x} - \boldsymbol{x}'| > \alpha h. \tag{3.11}$$

   The width of the compact support is defined by the smoothing width h and a scaling factor α. h and α determines the spread of the smoothing function.

3. $W(\boldsymbol{x} - \boldsymbol{x}') \geq 0$ for any point $\boldsymbol{x}'$. Minus sign density contribution from particles is unphysical.

4. The smoothing kernel value for a paritcle should be monotonically decreasing with the increase of the distance from the particle. This is based on the physical consideration in that nearer particle should have a larger influence on the concerned particle.

5. The smoothing kernel should satisfy the Dirac delta function condition as the smoothing width approaches zero (already stated)

6. The smoothing function should be an even function so that it does depend on only the distance between particles.

Several smoothing kernels satisfying these properties were developed. Among them, we typically use the smoothing kernels given below,

$$W(q,h) = \frac{\sigma}{h^\nu} e^{-q^2}, \tag{3.12}$$

where $q = r/h$ and the normalisation constant σ is $1/\sqrt(\pi)$, $1/\pi$ and $1(\pi\sqrt(\pi))$ in one-, two-, and three-dimensional space, respectively. Another example is given as

$$W(q,h) = \frac{\sigma}{h^\nu} \begin{cases} 1 - \frac{3}{2}q^2 + \frac{3}{4}q^3, & 0 \le q < 1 \\ \frac{1}{4}(2-q)^3 & 1 \le 1 < 2 \\ 0 & q \ge 2. \end{cases} \tag{3.13}$$

with normalisation $\sigma = [2/3, 10/(7\pi), 1/\pi]$.

In terms of these framework of SPH, the following ideal fluid dynamics equations,

$$\frac{\partial \rho}{\partial t} + \nabla \cdot (\rho \boldsymbol{u}) = 0, \tag{3.14a}$$

$$\rho(\frac{\partial \boldsymbol{u}}{\partial t} + (\boldsymbol{u} \cdot \nabla)\boldsymbol{u}) = -\nabla p, \tag{3.14b}$$

$$\frac{\partial \epsilon}{\partial t} + (\boldsymbol{u} \cdot \nabla)\epsilon = -\frac{p}{\rho}(\nabla \cdot \boldsymbol{u}), \tag{3.14c}$$

$$\epsilon = \frac{p}{(\gamma - 1)\rho}, \tag{3.14d}$$

where ρ is the mass density, $\boldsymbol{u}$ is the flow, p is the pressure, ϵ is the internal energy, and γ is the ratio of specific heats, can be discretized into a set of equations of N-particles,

$$\frac{d\rho_a}{dt} = \sum_b m_b \boldsymbol{v}_{ab} \nabla_a W_{ab}, \tag{3.15a}$$

$$\frac{d\boldsymbol{v}_a}{dt} = -\sum_b \left(\frac{p_b}{\rho_b^2} + \frac{p_a}{\rho_a^2} \right) \nabla_a W_{ab}, \tag{3.15b}$$

$$\frac{d\epsilon_a}{dt} = \left(\frac{p_a}{\rho_a^2} \right) \sum_b m_b \boldsymbol{v}_{ab} \cdot \nabla_a W_{ab}, \tag{3.15c}$$

$$\frac{d\boldsymbol{x}_a}{dt} = \boldsymbol{v}_a. \tag{3.15d}$$

Here, we employ a notation $\boldsymbol{v}_{ab} = \boldsymbol{v}_a - \boldsymbol{v}_b$ and $\boldsymbol{v}_a$ is the velocity of a particle a. Besides, $\boldsymbol{x}_a$ is the position of a quasi-particle a. These are the basic equations of SPH.

3.2 Hall-MHD using drift approximation

Ideal Hall-MHD is the model which neglects the electron inertia, because of its small mass, in the ideal two-fluid model. The set of equations are as follows:

$$\frac{dn}{dt} = -n\nabla \cdot \boldsymbol{u}, \tag{3.16a}$$

$$m_i n \frac{d\boldsymbol{u}_i}{dt} = en(\boldsymbol{E} + \boldsymbol{u}_i \times \boldsymbol{B}) - \nabla p_i, \tag{3.16b}$$

$$\boldsymbol{E} + \boldsymbol{u}_e \times \boldsymbol{B} + \frac{1}{en}\nabla p_e = 0, \tag{3.16c}$$

$$\nabla \times \boldsymbol{B} = \mu_0 \boldsymbol{j}, \tag{3.16d}$$

$$\frac{\partial \boldsymbol{B}}{\partial t} = -\nabla \times \boldsymbol{E}. \tag{3.16e}$$

Here, we assume that the displacement current can be neglected and the charge neutral condition $n_i = n_e = n$ is satisfied. Furthermore, the ideal plasma must be adiabatic, i.e,

$$p = C\rho^\gamma. \tag{3.17}$$

When electron mass is neglected, the fluid velocity $\boldsymbol{u}$ can be approximately expressed by the ion flow velocity $\boldsymbol{u}_i$, since $\boldsymbol{u} = (m_e\boldsymbol{u_e} + m_i\boldsymbol{u}_i)/(m_i + m_e) \simeq \boldsymbol{u}_i$. Besides, we know the relation

$$\boldsymbol{u}_e = \boldsymbol{u}_i - \boldsymbol{j}/(en) = \boldsymbol{u}_i - \nabla \times \boldsymbol{B}/(\mu_0 en). \tag{3.18}$$

Here, we mention the equation of motion of ions, eq. (3.16b), before performing the SPH discretization. The form of eq. (3.16b) resembles the equation of motion of the real ion particle. The apparent difference is just the gradient term of pressure. Although the quasi-particles and real particles are, of course, different, the quasi-particles are expected to gyrate around the magnetic field lines by the Lorentz force $\boldsymbol{u} \times \boldsymbol{B}$. Therefore, in the SPH for Hall-MHD, directly discretized from the set of eqs. (3.16), the gyro-motion

of quasi-particles may prevent from obtaining an efficient time step due to the microscopic time/space scale of gyro-motion, on the order of gyro-radius r_{Li} and gyro-frequency Ω_i, and extracting the interested bulk flow of plasma.

To avoid such inefficiency in a magnetized plasma, we develop a Hall-MHD model using drift approximation, that is, we get rid of the scale of ion's gyromotion from the full Hall-MHD model. The resultant drift Hall-MHD model is as follows:

$$\boldsymbol{u} = \frac{\boldsymbol{E} \times \boldsymbol{B}}{B^2}, \tag{3.19a}$$

$$\frac{d\boldsymbol{E}}{dt} = \frac{B^2}{m_i n}\boldsymbol{j}, \tag{3.19b}$$

$$\frac{d\boldsymbol{B}}{dt} = (\boldsymbol{u} \cdot \nabla)\boldsymbol{B} + \nabla \times \left[(\boldsymbol{u} - \frac{\boldsymbol{j}}{en}) \times \boldsymbol{B} \right] \tag{3.19c}$$

$$\nabla \times \boldsymbol{B} = \mu_0 \boldsymbol{j}, \tag{3.19d}$$

$$\frac{dn}{dt} = -n \nabla \cdot \boldsymbol{u}. \tag{3.19e}$$

As you recognize easily, the flow velocity $\boldsymbol{u}$ is the $E \times B$ drift and $\boldsymbol{j}$ is related to ion's polarization drift (electron's polarization drift is ignored by its small mass). The drift approximation is easily performed when the motion along the magnetic field lines are not conrerned, since, in such case, the drift motion across the magnetic field and the tangential motion are apparently decoupled. When the tangential motion is existed, the drift approximation may be complicated. At the present, we omitt the pressure, a driver of tangential motion, for simplicity. The reason why I made the simplification is as follows: we want to clarify mainly that the SPH method is capable to simulate the Hall-MHD model. If we can develop a SPH scheme for the simple drift Hall-MHD, we think that SPH for more general drift Hall-MHD model and full Hall-MHD are just a extention of the simple drift Hall-MHD. Therefore, although we may construct more general drift approximated Hall-MHD model in terms of ∇B drift or other drift, at first we use the model eqs. (3.19). To check the validity of this model, we will see a dispersion relation of shear Alfven wave in the next section.

3.3 Dispersion relation of drift Hall-MHD

Before proceeding the derivation of the dispersion relation, we normarize the Hall-MHD using drift approximation. The variables are normalized by

typical scale length L, appropriate measure of the magnetic field B_0 and density n_0 as

$$\boldsymbol{x} = L\tilde{\boldsymbol{x}}, \quad \boldsymbol{B} = B_0\tilde{\boldsymbol{B}}, \quad n = n_0\tilde{n}, \tag{3.20}$$

$$\boldsymbol{u} = V_A\tilde{\boldsymbol{u}}, \quad t = \tau_A\tilde{t} \tag{3.21}$$

The resultant normalized equations are as follows:

$$\tilde{\boldsymbol{u}} = \frac{\tilde{E}\times\tilde{\boldsymbol{B}}}{\tilde{B}^2}, \tag{3.22a}$$

$$\frac{d\tilde{\boldsymbol{E}}}{d\tilde{t}} = \frac{\tilde{B}^2}{\tilde{n}}\tilde{\boldsymbol{j}}, \tag{3.22b}$$

$$\frac{d\tilde{\boldsymbol{B}}}{d\tilde{t}} = (\tilde{\boldsymbol{u}}\cdot\tilde{\nabla})\cdot\tilde{\boldsymbol{B}} + \tilde{\nabla}\times\left[(\tilde{\boldsymbol{u}} - \delta_i\frac{\tilde{\boldsymbol{j}}}{\tilde{n}})\times\tilde{\boldsymbol{B}}\right], \tag{3.22c}$$

$$\tilde{\nabla}\times\tilde{\boldsymbol{B}} = \tilde{\boldsymbol{j}}, \tag{3.22d}$$

$$\frac{d\tilde{n}}{dt} = -\tilde{n}\tilde{\nabla}\cdot\tilde{\boldsymbol{u}}, \tag{3.22e}$$

where we introduced the symbol, $\delta_i = \lambda_i/L$. The variables with $\tilde{}$ are normalized. From here, we omit the $\tilde{}$ for simplicity. We linearize (3.22) about the uniform equilibrium $\boldsymbol{B}_0 = B_0\boldsymbol{e}_z$, $\boldsymbol{u} = \boldsymbol{E} = 0$ and $n = 1$, as

$$\boldsymbol{u} = \boldsymbol{u}_1, \tag{3.23a}$$

$$\boldsymbol{B} = \boldsymbol{B}_0 + \boldsymbol{B}_1, \tag{3.23b}$$

$$n = 1 + n_1, \tag{3.23c}$$

$$\boldsymbol{E} = \boldsymbol{E}_1, \tag{3.23d}$$

with perturbations proportional to $exp[i(\boldsymbol{k}\cdot\boldsymbol{x} - \omega t)]$. Substituting (3.23) into (3.22), we obtain

$$\boldsymbol{u}_1 = \frac{\boldsymbol{E}_1\times\boldsymbol{B}_0}{B_0^2}, \tag{3.24a}$$

$$-i\omega\boldsymbol{E}_1 = B_0^2\boldsymbol{j}_1, \tag{3.24b}$$

$$-i\omega\boldsymbol{B}_1 = i\boldsymbol{k}\times[(\boldsymbol{u}_1 - \delta_i\boldsymbol{j}_1)\times\boldsymbol{B}_0], \tag{3.24c}$$

$$-i\omega n = -i\boldsymbol{k}\cdot\boldsymbol{u}_1, \tag{3.24d}$$

$$i\boldsymbol{k}\times\boldsymbol{B}_1 = \boldsymbol{j}_1. \tag{3.24e}$$

We consider a wave travelling along the magnetic field lines, i.e., $\boldsymbol{k} = k\boldsymbol{e}_z$. Eqs. (3.24) can be written as

$$-i\omega \boldsymbol{E}_1 = V_A^2 i\boldsymbol{k} \times \boldsymbol{B}_1, \tag{3.25}$$

$$-i\omega \boldsymbol{B}_1 = i\boldsymbol{k} \times \left[-\boldsymbol{E} - iB_0 k\delta_i \boldsymbol{B}_1\right], \tag{3.26}$$

where $V_A = B_0^2$ is the Alfvén velocity in the normalized unit. Substituting (3.25) into (3.26), we obtain,

$$(\omega^2 - V_A^2 k^2)\boldsymbol{B}_1 = iV_A \delta_i k\omega(\boldsymbol{k} \times \boldsymbol{B}_1) \tag{3.27}$$

where Ω_i is the gyro-frequency of ions. x and y components of the above equation is given in the matrix form:

$$\begin{pmatrix} \omega^2 - V_A^2 k^2 & iV_A \delta_i k^2 \omega \\ -iV_A \delta_i k^2 \omega & \omega^2 - V_A^2 k^2 \end{pmatrix} \begin{pmatrix} B_x \\ B_y \end{pmatrix} = 0. \tag{3.28}$$

The dispersion relation is obtained by setting the determint of the matrix in eq(3.28) to be zero, therefore we derive

$$\omega^2 - V_A^2 k^2 = \pm \delta_i V_A \omega k^2 \tag{3.29}$$

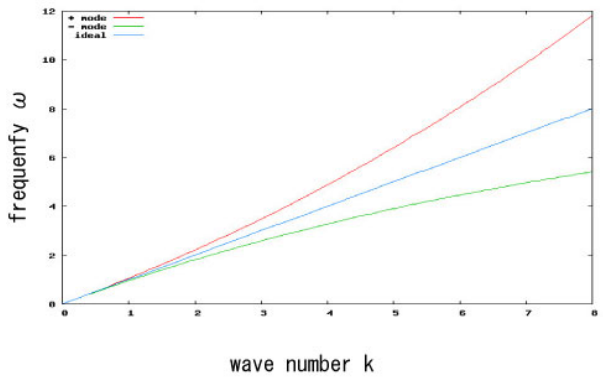

Figure 3.2: Dispesion relation of the shear Alfvén wave (+ mode, - mode, ideal)

This is consistent with the dispersion relation derived from full Hall-MHD model. Therefore, at least for the shear Alfvén wave, this Hall-MHD using drixt approximation is valid.

3.4 SPH form of drift Hall-MHD

Here we discretize the drift Hall-MHD equations by procedures of SPH. The basis of SPH for drift Hall-MHD is also the discretized expression of the density field $n(\boldsymbol{x}, t)$ (same as mass density ρ when we set the ion mass to 1),

$$n(\boldsymbol{x}, t) = \sum_b n_b W(\boldsymbol{x} - \boldsymbol{x}_b), \tag{3.30}$$

where n_b is the density and $\boldsymbol{x}_b$ is the position of the quasi-particle b and W is the smoothing kernel disscussed in section 3.1. In the SPH for drift Hall-MHD, quasi-particles move in a computational domain with charges B_b, E_b, j_b, v_b, n_b and $m_b = n_b \Delta V$.

The continuity equation can be replaced by the interpolant

$$\frac{dn_a}{dt} = \sum_b m_b \boldsymbol{v}_{ab} \nabla_a W_{ab} \tag{3.31}$$

where the notaiton $\boldsymbol{v}_{ab} = \boldsymbol{v}_a - \boldsymbol{v}_b$ has been used. This determines the time evolution of the information about the density carried by the quasi-particle a. In a similar way, (3.22b) can be written for the particle a in the form

$$\frac{d\boldsymbol{E}_a}{dt} = \frac{B_a^2}{n_a} \boldsymbol{j}_a. \tag{3.32}$$

Also, the velocity of the particle a is given by

$$\boldsymbol{v}_a = \frac{\boldsymbol{E}_a \times \boldsymbol{B}_a}{B_a^2}. \tag{3.33}$$

Next, we consider the evaluation of $\boldsymbol{j}_a$, the current density carried by the particle a, in SPH. Equation (3.22d) is rewritten as

$$j^i = \epsilon^{ijk} \frac{\partial}{\partial x^j} B^k \tag{3.34}$$

$$= \epsilon^{ijk} \frac{1}{n} \left[\frac{\partial}{\partial x^j} (n B^k) - B^k \frac{\partial n}{\partial x^j} \right]. \tag{3.35}$$

This can be written for the particle a,

$$j_a^i = \epsilon^{ijk} \left[\frac{1}{n_a} \sum_b m_b B_b^k \nabla_j W_{ab} - \frac{B_a^k}{n_a} \sum_b m_b \nabla_j W_{ab} \right]. \tag{3.36}$$

Equation (3.36) can be written in the vector form as

$$\boldsymbol{j}_a = \frac{1}{n_a}\sum_b (\boldsymbol{B}_a - \boldsymbol{B}_b) \times \nabla_a W_{ab}. \tag{3.37}$$

Next, we consider the SPH discretization of eq. (3.22c). Equation (3.22c) can be rewritten as

$$\frac{d\boldsymbol{B}}{dt} = (\boldsymbol{u}\cdot\nabla)\boldsymbol{B} - \nabla\times\boldsymbol{E} + \frac{\delta_i}{n^2}\nabla n \times (\boldsymbol{j}\times\boldsymbol{B}) - \frac{\delta_i}{n}\nabla\times(\boldsymbol{j}\times\boldsymbol{B}). \tag{3.38}$$

Equation (3.38) can be transformed into another form and written in terms of the component denotation as

$$\frac{dB^i}{dt} = u^k\frac{\partial B^i}{\partial x^k} - \epsilon^{ijk}\frac{1}{n}\left(\frac{\partial}{\partial x^j}(nE^k) - E^k\frac{\partial n}{\partial x^j}\right) + \frac{\delta_i}{n^2}\left[\nabla n\times(\boldsymbol{j}\times\boldsymbol{B}\right]^i - \frac{\delta_i B^k}{n^2}\left(\frac{\partial}{\partial x^k}(nj^i) - j^i\frac{\partial n}{\partial x^k}\right). \tag{3.39}$$

Here, we used the vector identity,

$$\nabla\times(\boldsymbol{A}\times\boldsymbol{B}) = \boldsymbol{A}(\nabla\cdot\boldsymbol{B}) - \boldsymbol{B}(\nabla\cdot\boldsymbol{A}) + (\boldsymbol{B}\cdot\nabla)\boldsymbol{A} - (\boldsymbol{A}\cdot\nabla)\boldsymbol{B}. \tag{3.40}$$

For the simple case, where $\nabla n = 0$ and $\boldsymbol{u}\cdot\nabla = 0$ (realized in the Alfven wave travelling along the magnetic field line), Equation (3.40) can be written for the particle a,

$$\frac{dB_a^i}{dt} = -\epsilon^{ijk}\frac{1}{n_a}\left(\sum_b m_b E_b^k\nabla_j W_{ab} - E_a^k\sum_b m_b\nabla_j W_{ab}\right) - \frac{\delta_i B_a^k}{n_a^2}\left(\sum_b m_b j_b^i\nabla_k W_{ab} - j_a^i\sum_b m_b\nabla_k W_{ab}\right). \tag{3.41}$$

Equation (3.41) can be written in the vector notation as

$$\frac{d\boldsymbol{B}_a}{dt} = \frac{1}{n_a}\sum_b m_b(\boldsymbol{E}_b - \boldsymbol{E}_a)\times\nabla W_{ab} + \frac{\delta_i}{n_a^2}\sum_b m_b(\boldsymbol{j}_a - \boldsymbol{j}_b)(\boldsymbol{B}_a\cdot\nabla)W_{ab}. \tag{3.42}$$

Here, we summarize the set of equations which determine the time evo-

lution of the particle a. These are as follows:

$$\frac{dn_a}{dt} = \sum_b m_b \boldsymbol{v}_{ab} \nabla_a W_{ab}, \tag{3.43a}$$

$$\frac{d\boldsymbol{E}_a}{dt} = \frac{B_a^2}{n_a} \boldsymbol{j}_a, \tag{3.43b}$$

$$\boldsymbol{v}_a = \frac{\boldsymbol{E}_a \times \boldsymbol{B}_a}{B_a^2}, \tag{3.43c}$$

$$\boldsymbol{j}_a = \frac{1}{n_a} \sum_b (\boldsymbol{B}_a - \boldsymbol{B}_b) \times \nabla_a W_{ab}, \tag{3.43d}$$

$$\frac{d\boldsymbol{B}_a}{dt} = \frac{1}{n_a} \sum_b m_b (\boldsymbol{E}_b - \boldsymbol{E}_a) \times \nabla W_{ab} \tag{3.43e}$$

$$+ \frac{\delta_i}{n_a^2} \sum_b m_b (\boldsymbol{j}_a - \boldsymbol{j}_b)(\boldsymbol{B}_a \cdot \nabla) W_{ab}, \tag{3.43f}$$

$$\frac{d\boldsymbol{x}_a}{dt} = \boldsymbol{v}_a. \tag{3.43g}$$

3.5 1-D simulation of shear Alfvén wave

3.5.1 Configuration and basic equations

Here we simulate the shear Alfvén wave, especially traveling along the magnetic field lines, in one-dimensional configuration using SPH for the drift Hall MHD developed in the previous section as a benchmark. We check that a dispersion relation derived from the numerical simulation agrees with the analytic solution. The configuration is shown in Fig. 3.3.

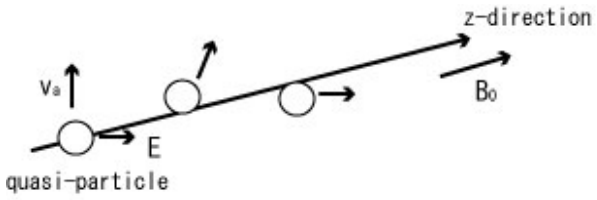

Figure 3.3: Schematic view of the configuration of 1-D Alfvén wave simulation.

Now, a back ground magnetic field line lies toward the z-direction. For the shear Alfvén wave, the motion of quasi-particles is almost limited in the

x-y plane, since the motion along the z-direction is generated by the second order quantity $\boldsymbol{E}_1 \times \boldsymbol{B}_1$. Therefore, we ignore the motion in the z-direction and particles does not change their position in the z-direction. In this case, each particle moves in the x-y plane with changing the charge quantities, B_x, B_y, E_x, E_y, j_x and j_y. Since the x and y direction is homogeneous, we just concern the differentiation along the z-direction. Specific form of equations for particle a are as follows:

$$v_a^x = \frac{E_a^y}{B_0}, \qquad v_a^y = -\frac{E_a^x}{B_0}, \tag{3.44a}$$

$$\frac{dE_a^x}{dt} = \frac{B_0^2}{n_a} j_a^x, \qquad \frac{dE_a^y}{dt} = \frac{B_0^2}{n_a} j_a^y, \tag{3.44b}$$

$$j_a^x = \frac{1}{n_a} \sum_b m_b (B_a^y - B_b^y) \frac{\partial W_{ab}}{\partial z}, \tag{3.44c}$$

$$j_a^y = -\frac{1}{n_a} \sum_b m_b (B_a^x - B_b^x) \frac{\partial W_{ab}}{\partial z}, \tag{3.44d}$$

$$\frac{dB_a^x}{dt} = \frac{1}{n_a} \sum_b m_b (E_b^y - E_a^y) \frac{\partial W_{ab}}{\partial z} + \frac{\delta_i B_0}{n_a^2} \sum_b m_b (j_a^x - j_b^x) \frac{\partial W_{ab}}{\partial z}, \tag{3.44e}$$

$$\frac{dB_a^y}{dt} = -\frac{1}{n_a} \sum_b m_b (E_b^x - E_a^x) \frac{\partial W_{ab}}{\partial z} + \frac{\delta_i B_0}{n_a^2} \sum_b m_b (j_a^y - j_b^y) \frac{\partial W_{ab}}{\partial z} \tag{3.44f}$$

where $\partial W_{ab}/\partial z = \partial W/\partial z|_{z=z_a-z_b}$. Besides, we employ a smoothing kernel as

$$W(\boldsymbol{x}_a - \boldsymbol{x}_b) = \frac{1}{h\sqrt{\pi}} exp(-[(x_a - x_b)^2 + (y_a - y_b)^2 + (z_a - z_b)^2]/h^2) \tag{3.45}$$

where h is a parameter, which is the typical distance between particles.

3.5.2 Procedure of numerical scheme

Here, we discuss the procedure of time stepping in the simulation code. Because the SPH algorithm reduces the original continuous partial differential equations to a set of ordinary differential equations, any stable time stepping algorithm for ordinary differential equations can be used. In our numerical code, we employ the second order Runge-Kutta method, assuring the second-order accuracy in time.

A schematic picture of time integration processes is shown in Fig. 3.4. Firstly, we integrate $\boldsymbol{B}$, $\boldsymbol{E}$, $\boldsymbol{v}$ and $\boldsymbol{x}$ for half step in terms of the present

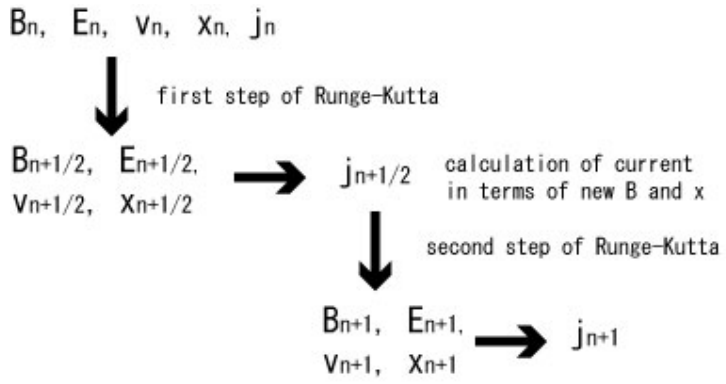

Figure 3.4: A schematic picture of time integration processes.

value. Then, we evaluate the current density on the time proceeded by half step in terms of renewed variables. Furthermore, we just take the same step in the second step of Runge-Kutta method. We set the time step of integration Δt sufficiently small not to disturb the Courant condition, $\Delta x/\Delta t > v$(phase speed).

3.5.3 initial conditions, parameters and boundary conditions

Since we want to derive a dispersion relation of the shear Alfvén wave, we input the eigen vectors of the shear Alfvén wave as a initial conditions and we obtain a phase velocity from a moving distance of a crest of the wave. The specific form of the initial condition for the + branch (fast mode) of the shear Alfvén wave is the following:

$$B_x = -0.001cos(k_z x), \tag{3.46}$$

$$B_y = 0.001sin(k_z x), \tag{3.47}$$

$$E_x = \frac{k_z B_0^2}{\omega_+} B_y, \tag{3.48}$$

$$E_y = -\frac{k_z B_0^2}{\omega_+} B_x, \tag{3.49}$$

$$n = 1.0, \tag{3.50}$$

where ω_+ is defined as

$$\omega_+ = B_0 \frac{\delta_i k_z^2 + k_z \sqrt{\delta_i^2 k_z^2 + 4}}{2}. \tag{3.51}$$

Similarly, initial conditions for the - brach (slow mode) are given by

$$B_x = 0.001 cos(k_z x), \tag{3.52}$$

$$B_y = 0.001 sin(k_z x), \tag{3.53}$$

$$E_x = \frac{k_z B_0^2}{\omega_-} B_y, \tag{3.54}$$

$$E_y = -\frac{k_z B_0^2}{\omega_1} B_x, \tag{3.55}$$

$$n = 1.0, \tag{3.56}$$

where ω_- is defined as

$$\omega_- = B_0 \frac{k_z \sqrt{\delta_i^2 k_z^2 + 4} - \delta_i k_z^2}{2}. \tag{3.57}$$

Initial conditions for the velocity and the current density are obtained from eqs. (3.43c) and (3.43d) consistently.

The important parameter in SPH is α, which determines the compact support area. In our simulation, α is set to 2, the value frequently used in other SPH studies. System size is ranged from 1 to 2, corresponding to the wave number initially injected. In responce to a change of the system size, we change particle numbers to keep certain accuracy: the characteristic paritlce distance Δx is maintained as the order of 10^{-2}. The parameter δ_i, the measure of the Hall-effect, is set to 0.5 or 0.1.

3.5.4 Numerical Results

A representative example of simulations is given in Fig. 3.5. The simulation in Fig. 3.5 is performed with paremeters, particle numbers N = 400, system size L = 2.0, wave number $k = 3\pi$ and $\delta_i = 0.1$. The slow mode is tracked in Fig. 3.5. We plot the x-component of the velocity v_x, the x-componet of the magnetic field B_x, the x-component of the current density j_x and the x-component of the electric field E_x. The wave seems to be traveling correctly

and the amplitude is well maintained. The changing rate of the amplitude per τ_A, the period time $2\pi/(kV_A)$, is less than 1% .

We plot the dispersion relation derived from numerical simulations with analytical solutions in Fig. 3.6. As we recognize from the Fig. 3.6, the dispersion relation for fast mode and slow mode is departed from the dispersion relation of ideal shear Alfven wave due to the Hall-effect. The dispersion relation obtained numerically is considerably identical to the analytic one and the data agreement is independent of the strength of the Hall effect.

Therefore, we can conclude that SPH for the Hall-MHD using drift approximation works well, at least in the linear regime.

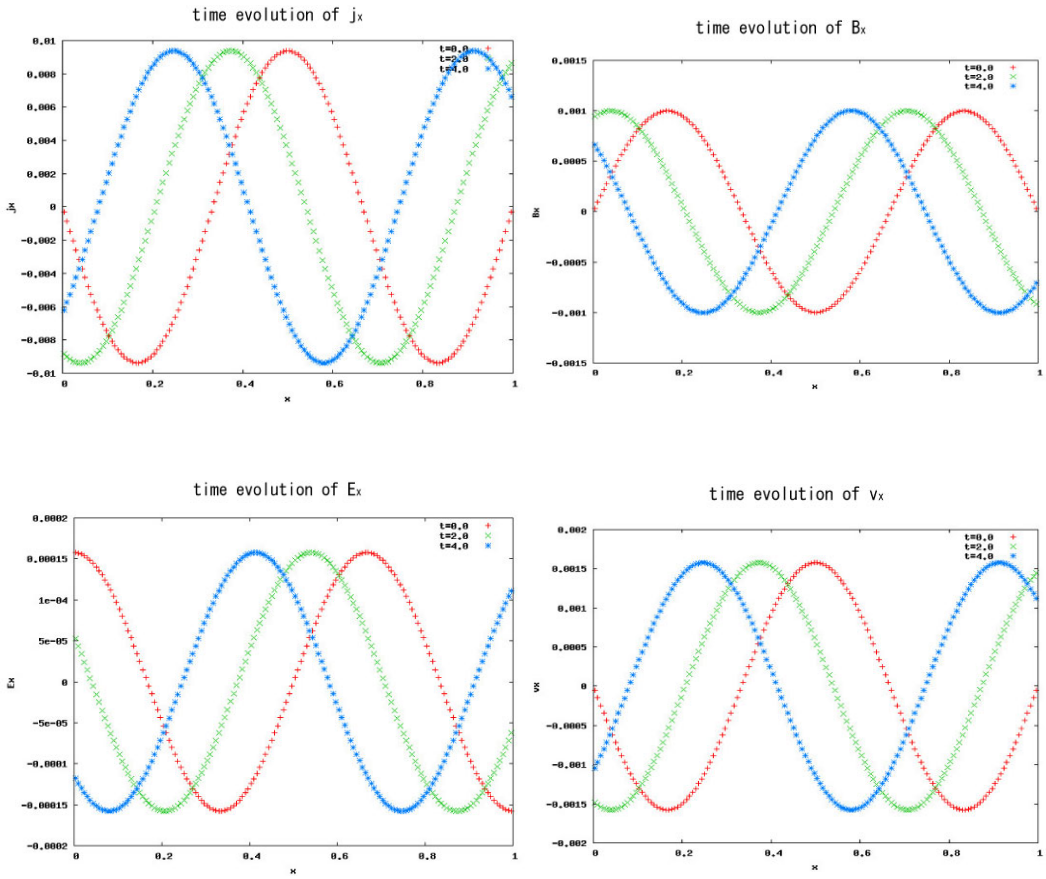

Figure 3.5: The picture of travelling Alfvén wave ($\delta_i = 0.1$, - branch).

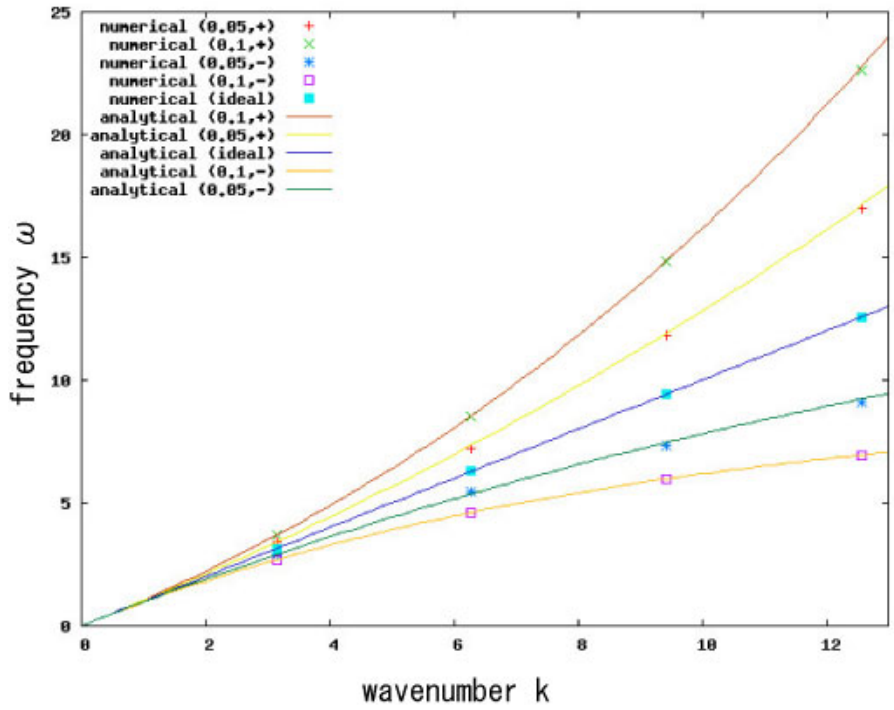

Figure 3.6: Dispersion relation derived numerically and analytically.

Chapter 4

Smoothed Particle Hydrodynamics for Langmuir wave

In the SPH for Hall-MHD discussed in Chap. 3, due to the drift approximation and neglection of the pressure, we did not take into account the quasi-particle's motion along the magnetic field lines. In the dynamics of plasma fluids, a typical driver of the motion along the magnetic field lines is the pressure, which features the difference between quasi-particles, expressing the continuous field as a collection of discretized points, and real particles. Therefore, here, we develop a SPH scheme, which include the effect of the pressure and simulate the electron-plasma wave (or the Langmuir wave), one of the electrostatic ($\boldsymbol{k} \times \boldsymbol{E} = 0$) waves travelling along the magnetic field, as a benchmark of the numerical scheme. Actually, we may be possible to treat the pressure as an extension of the SPH for drift Hall-MHD, however, in that case, a coupling between compressible modes, induced by the pressure, and imcompressible modes, such as shear Alfvén wave, makes it difficult to investigate the effect of pressure.

4.1 Electron plasma (Langmuir) wave

Here, we introduce the electron plasma wave briefly. If the electrons in a plasma are displaced from an uniform background of ions, electric fields will be built up in such a direction as to restore the charge neutrality of the plasma

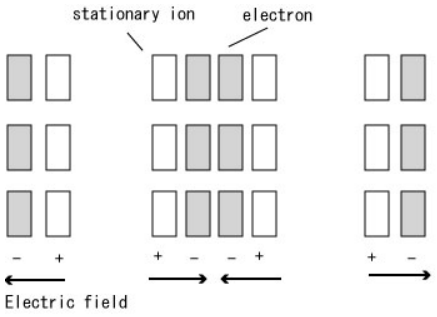

Figure 4.1: Schematic picture of plasma oscillation.

by pulling the electrons back to their original positions. Because of their inertia, the electrons will overshoot and oscillate around their equilibrium positions with the characteristic frequency ω_{pe}. This oscillation is so fast that massive ions cannot respond to the oscillating field and can be considered as fixed. In Fig. 4.1, the white rectangles represent typical elements of the ion fluid, and the displaced darkened rectangles are elements of the electron fluid. The resulting charge separation causes a spatially periodic $\boldsymbol{E}$ field, which tends to restore the electrons to their original positions. Langmuir oscillations do not propagate in a stationary cold plasma, as can be seen from the fact that the group velocity $v_g = \partial\omega/\partial k$ is zero. However, as we will see later, Langmuir waves have a phase velocity, even though they do not propagate.

Plasma oscillation can be propageted by thermal motion or the pressure. To see this feature, we shall derive an expression for electron plasma wave on the following assumptions:(1) plasma motion and a direction of propagation is parallel to the magnetic field lines (the x-direction); (2) the ions are fixed in space in an uniform distribution; (4) the plasma is infinite. As a consequence of assumptions, we have

$$\nabla = \boldsymbol{e}_x \frac{\partial}{\partial x}, \quad \boldsymbol{E} = E_x \boldsymbol{e}_x, \quad \nabla \times \boldsymbol{E} = 0, \quad \boldsymbol{E} = -\nabla\phi \tag{4.1}$$

A set of equations describing Langmuir wave is as follows:

$$m_e n_e \left[\frac{\partial \boldsymbol{u}_e}{\partial t} + (\boldsymbol{u}_e \cdot \nabla)\boldsymbol{u}_e \right] = -e n_e \boldsymbol{E} - \nabla p_e, \tag{4.2a}$$

$$\frac{\partial n_e}{\partial t} + \nabla \cdot (n_e \boldsymbol{u}_e) = 0, \tag{4.2b}$$

$$\nabla \cdot \boldsymbol{E} = \frac{\partial E_x}{\partial x} = \frac{e}{\epsilon_0}(n_i - n_e), \tag{4.2c}$$

$$p_e = C n_e^{\gamma}. \tag{4.2d}$$

Linearizing about a stationary equilibrium, $n = n_0$ and $\boldsymbol{u} = \boldsymbol{E} = 0$, with perturbed quantities n_1, $\boldsymbol{u}_1$ and $\boldsymbol{E}_1$. We assume that the perturbed quantities have a form as

$$A_1 = A_1 exp[i(\boldsymbol{k} \cdot \boldsymbol{x} - \omega t)] \tag{4.3}$$

Equations (4.2a)-(4.2c) now become

$$-im\omega n_0 u_1 = -e n_0 E_1 - \gamma T_e i k n_1, \tag{4.4}$$

$$-i\omega n_1 = -n_0 i k u_1, \tag{4.5}$$

$$ik\epsilon_0 E_1 = -e n_1, \tag{4.6}$$

where we used the relation $p = nT$. From the above equations, we obtain a dispersion relation,

$$\omega^2 = \omega_{pe}^2 + \frac{\gamma}{2} k^2 v_{th,e}^2, \tag{4.7}$$

where $v_{th,e}^2 = 2T_e/m_e$. As you see from the equation (4.7), the pressure generates the dispersion for the Langmuir wave.

4.2 SPH for electron plasma wave

To simulate electron plasma wave, concerning the motion parallel to the magnetic field lines, by SPH, we discretize basic equations of electron plasma wave (4.2). For the case of electron plasma wave, quasi-particles distribute along the x-direction. The quasi-particle a moves along x-direction at the velocity $\boldsymbol{v}_a$ with charges, such as the density n_a, the electric field $\boldsymbol{E}_a$, the pressure P_a and the electrostatic potential ϕ_a. Before proceeding the discretization,

we introduce a normalization unit. Variables are normalized by the Debye length λ_D, the electron thermal velocity $v_{th,e}$ and typical density n_0, as

$$n_e = n_0 \tilde{n_e}, \quad \boldsymbol{u}_e = v_{th,e}\tilde{\boldsymbol{u}}_e, \quad (1/dt) = \omega_{pe}(1/d\tilde{t}), \tag{4.8}$$

$$\nabla = (1/\lambda_D)\tilde{\nabla}, \quad \boldsymbol{E} = (en_0\lambda_D/\epsilon_0)\tilde{\boldsymbol{E}}, \quad p_e = m_e n_0 v_{th,e}^2 \tilde{p_e}. \tag{4.9}$$

The resultant normalized equations in one-dimensional configuration are as follows:

$$\frac{du^x}{dt} = \frac{\partial\phi}{\partial x} - \frac{1}{n}\frac{\partial p}{\partial x}, \tag{4.10a}$$

$$\frac{dn}{dt} = -n\frac{\partial u^x}{\partial x}, \tag{4.10b}$$

$$\frac{\partial^2\phi}{\partial x^2} = -(1-n), \tag{4.10c}$$

$$p = Dn^\gamma, \tag{4.10d}$$

where we omitted the subscript e and $\tilde{}$ for simplicity. The continuity equation for the particle a can be written as

$$\frac{dn_a}{dt} = n_a \sum_b \frac{m_b}{n_b}(v_a^x - v_b^x)\frac{\partial}{\partial x_a}W_{ab}, \tag{4.11}$$

where $W_{ab} = W(x_a - x_b, h)$ is the smoothing kernel, discussed in the previous chapter. The equation of motion for the particle a can be written as

$$\frac{dv_a^x}{dt} = -E_a^x - \sum_b m_b \left(\frac{p_b}{n_b^2} + \frac{p_a}{n_a^2}\right)\frac{\partial}{\partial x_a}W_{ab}, \tag{4.12}$$

where the pressure term is evaluated as

$$\frac{1}{n}\frac{\partial p}{\partial x} = \frac{\partial}{\partial x}\left(\frac{p}{n}\right) + \frac{p}{n^2}\frac{\partial n}{\partial x} \tag{4.13}$$

$$\rightarrow \sum_b m_b \frac{p_b}{n_b^2}\frac{\partial}{\partial x_a}W_{ab} + \frac{p_a}{n_a^x}\sum_b m_b \frac{\partial}{\partial x_a}W_{ab}. \tag{4.14}$$

This form of the pressure term is known to preserve the momentum conservation laws. The electric field carried by the particle a can be given by

$$E_a^x = \sum_b m_b(\phi_a - \phi_b)\frac{\partial}{\partial x_a}W_{ab}. \tag{4.15}$$

Besides, the velocity of the particle a is related to the time derivative of its position, i.e.,

$$\frac{dx_a}{dt} = v_a^x \tag{4.16}$$

Finally, we mention the estimation of the electrostatic potential ϕ_a. In the SPH for Langmuire wave, we have no time evolution equation of the electric field or the related electrostatic potential. The conventional SPH is applied to solve N-body problems with self gravity, then, they have to solve the Poisson's equation with respect to the gravity potential,

$$\nabla^2 V(\boldsymbol{x}) = -4\pi G\rho(\boldsymbol{x}), \tag{4.17}$$

where $V(\boldsymbol{x})$ is the gravity potential and $\rho(\boldsymbol{x})$ is the mass density. In the SPH, this Poisson equation is solved by

$$V(\boldsymbol{x}) = \sum_b G\rho_b \frac{(\boldsymbol{x} - \boldsymbol{x}_b)}{|\boldsymbol{x} - \boldsymbol{x}_b|^3}. \tag{4.18}$$

However, this estimation can not apply one-dimensional problems, since the potential does not fall as the distance incereases. Therefore we solve the Poisson's equation by finite difference method in terms of non-uniform grids where particles are situated,

$$\frac{d^2\phi}{dx^2} = -\frac{\rho(x_a)}{\epsilon_0} \qquad \rho : \text{the charge density.} \tag{4.19}$$

We summarize the SPH equations of the particle a for Langmuir wave simulation.

$$\frac{dn_a}{dt} = n_a \sum_b \frac{m_b}{n_b}(v_a^x - v_b^x)\frac{\partial}{\partial x_a}W_{ab}, \tag{4.20a}$$

$$\frac{dv_a^x}{dt} = -E_a^x - \sum_b m_b \left(\frac{p_b}{n_b^2} + \frac{p_a}{n_a^2}\right)\frac{\partial}{\partial x_a}W_{ab}, \tag{4.20b}$$

$$E_a^x = \sum_b m_b(\phi_a - \phi_b)\frac{\partial}{\partial x_a}W_{ab}, \tag{4.20c}$$

$$\frac{dx_a}{dt} = v_a^x, \tag{4.20d}$$

$$p_a = Dn_a^\gamma, \tag{4.20e}$$

$$\frac{d^2\phi(x_a)}{dx^2} = n_a - 1. \tag{4.20f}$$

In the next section, we will mention an numerical scheme for solving the Poisson equation.

4.3 Poisson solver

Here, we mention the finite difference method using non-uniform grids. We can obtain the formula to approximate differentiation by finite difference using the Taylor expansion. As an example, we consider an approximation of the second-order derivative d^2u/dx^2 at a point i, in terms of values evaluated at three points $i-1$, i and $i+1$.

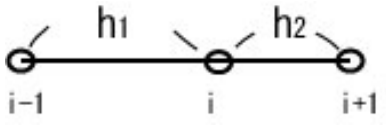

Figure 4.2: Difference approximation of second-order derivative.

The second-order derivative at the point i can be written as

$$\left.\frac{d^2u}{dx^2}\right|_i \simeq \frac{2u_{i-1}}{h_1(h_1+h_2)} - \frac{2u_i}{h_1h_2} + \frac{2u_{i+1}}{h_2(h_1+h_2)}, \tag{4.21}$$

where this expression assures the second-order accuracy in h.

Using the finite difference approximation (4.21), the Poisson's equation with periodic boundary condition can be tranformed into a matrix form as

$$A \cdot B = C, \tag{4.22}$$

where

$$A = \begin{pmatrix} a_{11} & a_{12} & \dots & & & a_{1n} & 0 \\ a_{21} & a_{22} & a_{23} & \dots & & & 0 \\ 0 & a_{32} & a_{33} & a_{34}\cdots & & & 0 \\ & \vdots & \vdots & \vdots & & & \\ & & & & a_{NN-1} & a_{NN} & a_{NN+1} \\ 0 & \cdots & \cdots & & & & 1 \end{pmatrix}, \tag{4.23}$$

$$B = {}^t\begin{pmatrix} \phi_1 & \phi_2 & \cdots & \cdots & \phi_N & \phi_{N+1} \end{pmatrix}, \tag{4.24}$$

$$C = {}^t\begin{pmatrix} -\rho_1 & -\rho_2 & \cdots & \cdots & -\rho_N & D \end{pmatrix}. \tag{4.25}$$

The matrix A is a little bit modified from a triple diagonal matrix due to the boundary condition, for example, where a_{1n} appeares.

The vector B, the discretized potential, can be obtaind as

$$B = A^{-1} \cdot C. \tag{4.26}$$

4.4 Numerical implementation

We will discuss a procedure of time step similarly, as we did in Chap. 3. We employ the second-order Runge-Kutta method about time integration and the second-order finite difference approximation discussed in the previous section for spatial derivative.

A schematic picture of time integration processes is shown in Fig. 4.3. We first integrate $\boldsymbol{x}_a$, $\boldsymbol{v}_a$, n_a and p_a for half step in terms of the present values. Then, we solve the Poisson's equation using the renewed density n_a and $\boldsymbol{x}_a$. Furethermore, we obtain $E_{n+1/2}$ by differentiation of renewed electrostatic potential $\phi_{n+1/2}$. Repeating the same procedures again, we finish a sequence of a time step and derive the quantities on the proceeded time.

4.5 Initial conditions, parameters and boundary conditions

Firstly, we mention the initial condition. We input the eigen vectors of electron plasma wave, since we want to see a dispersion relation. As in the case of SPH for Hall-MHD, a phase velocity is obtained from a moving distance of a crest of the wave. The specific form of the initial condition is

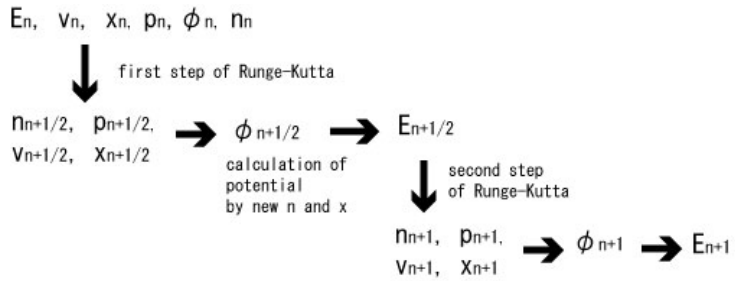

Figure 4.3: A schematic picture of a time integration processes performed in SPH for Langmuir wave.

the following:

$$n = 1.0 + 0.01sin(kx), \tag{4.27}$$

$$v = \frac{\omega_p}{k_x}0.01sin(kx), \tag{4.28}$$

$$\phi = -\frac{1}{k_x^2}0.01sin(kx). \tag{4.29}$$

Initial conditions for other variables are obtained consistently in the numerical scheme.

We performed several cases with changing the wave number k and the parameter D, determining the measure of the pressure effect. According to the change of the simulating situation, the system length L and particle numbers N is also changed to keep desired numerical accuracy. Number of particles contained in a wave packet is order of 10^2.

We employ the periodic boundary condition for all simulations perfomed in this chapter.

4.6 Numerical results

We simulate the propagation of the Langmuir wave in 1-D configuration. A typical time development of the wave is shown in Fig. 4.4. We distributed 800 particles for the simulation shown in Fig. 4.4, with parameters, D = 0.001 and $k = 4\pi$, where D expresses the measure of the pressure. As we see from Fig. 4.4, the wave seems to propagate properly.

The dispersion relation obtained numerically and analytically is shown in Fig. 4. 5. It seems that the dispersion relation obtained numerically almost agrees with the analytic one. The error about 2% is occured for the case that the pressure effect is strong, where the pressure coefficient D = 0.1. Furthermore, there is a tendency that phase velocities obtained numerically are larger than the analytic phase velocities. Since we aim to incorporate the pressure correctly, we mention the error of the dispersion relation carefully.

In Fig. 4.6, we plotted the ratio between the phase velocity deviation from the analytic solution and the analytic phase velocity, that is, $|v_{ph} - \tilde{v_{ph}}|/\tilde{v_{ph}}$, where $\tilde{v_{ph}}$ expresses the analytic phase velocity, for several pressure coefficients D. As we recognize, the ratio increases as the pressure coefficient increases, although its magnitude is still small.

The reason why the error increases with increase of the pressure coefficient is as follows: we estimate the pressure carried by the quasi-particle a as $D\rho_a^\gamma$ in this SPH scheme. Actually, this is not the same as the conventional SPH. In the conventional SPH, the pressure p_a is estimated as $(\gamma-1)\rho_a\epsilon_a$, where ϵ_a is the internal energy carried by the particle a. The internal energy carried by the particle a is obtained as

$$\frac{d\epsilon_a}{dt} = \left(\frac{p_a}{\rho_a^2}\right) \sum_b m_b \boldsymbol{v}_{ab} \cdot \nabla_a W_{ab}. \tag{4.30}$$

Therefore, the resultant pressure is affected by the smoothing of the internal energy as well as the smoothing of the density in the conventional SPH scheme. Here, we employed the simple derivation of the pressure because the formal derivation of the pressure is time-consuming due to solving the ordinary differential equation about ϵ_a. Thus, if we use the relation (4.30), we can obtain more accurate effecte of the pressure. The tendency that phase velocity obtained numerically is larger than the analytice one can be also explained by the same reason, that is, the pressure, which is weakly smoothed, leads to overestimation of the pressure force and produces larger phase velocities.

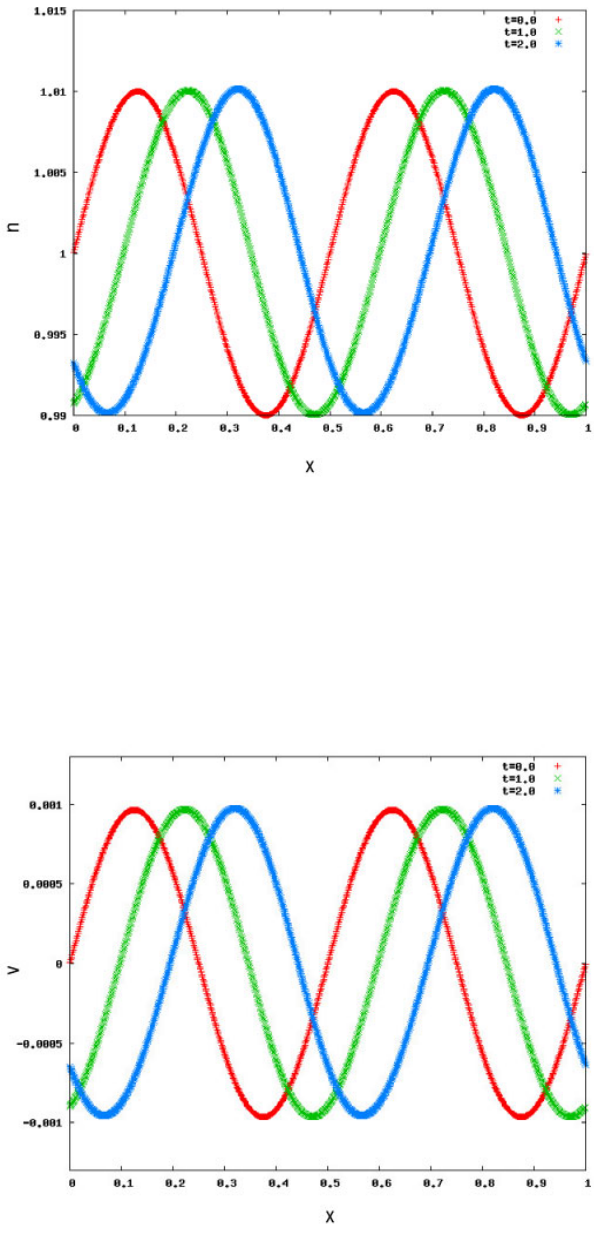

Figure 4.4: A picture of propagating Langmuir wave ($k = 4\pi$, D=0.001, $\gamma = 3.0$).

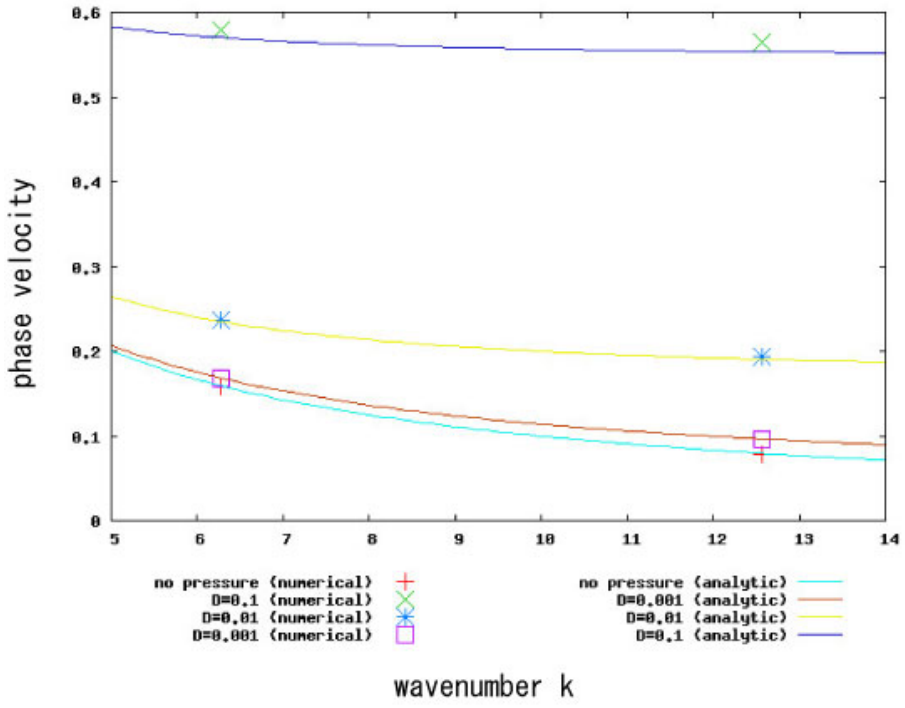

Figure 4.5: Dispersion relation obtained numerically and analytically for cases, D=0.0, D=0.001, D=0.01 and D=0.1.

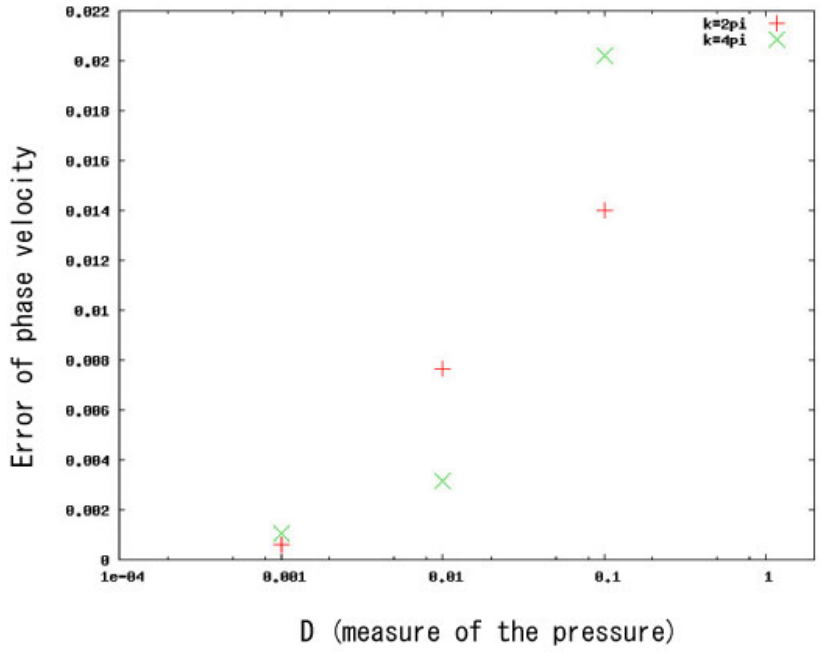

Figure 4.6: The error of the phase velocity: we plotted $|v_{ph} - \tilde{v_{ph}}|/\tilde{v_{ph}}$ for D=0.001, D=0.01 and D=0.1, where $\tilde{v_{ph}}$ is the phase velocity derived analytically.

Chapter 5

SPH simulation of ion acoustic wave

In Chap. 3, we developed the SPH scheme for Hall-MHD using drift approximation. We run the one-dimensional simulation of shear Alfvén wave propagating along the magnetic field lines, as a typicall example of transverse waves and check whether the numerical dispersion relation agrees with the analytic dispersion relation. In the previous chapter, we developed the SPH scheme which can simulate the motion along the magnetic field lines and run the one-dimensional simulation of Langmuir wave as a benchmark of the scheme. The dispersion relation obtained numerically agrees with the analytical one.

However, at this moment, we do not assure that the developed SPH shemes works in the non-linear regime. Thus, in this chapter, we run a simulation of non-linear wave. Particularly, we simulate a stable propagation of ion acoustic soliton. A soliton is a solitary wave caused by a delicate balance between nonlinear and dispersive effects in the medium. Ion acoustic wave is one of the longitudinal waves as is the case with Langmuir wave. The model equations to describe ion acoustic wave in a normalized form resemble the equations for Langmuir wave. The difference just appeares in the source term of Poisson's equation. Therefore, the numerical scheme for ion acoustic wave is obtained by a little modification of the SPH scheme for Langmuir wave.

5.1 Ion acoustic wave

Here, we discuss how to describe the ion acoustic wave briefly. The ion-acoustic wave is one of the most important waves in plasma physics since it is used as the basis for a theory of non-magnetic collisionless shock waves. The basic equations describing the ion acoustic wave are as follows: the ion motion in high temperature electrons, subject to the Boltzmann distribution, is determined by

$$-eE - \frac{T_e}{n_e}\frac{\partial n_e}{\partial x} = 0, \tag{5.1a}$$

$$\frac{\partial n_i}{\partial t} + \frac{\partial}{\partial x}(n_i u_i) = 0, \tag{5.1b}$$

$$\frac{\partial u_i}{\partial x} + u_i\frac{\partial u_i}{\partial x} = \frac{e}{m_i}E, \tag{5.1c}$$

$$\frac{\partial E}{\partial x} = \frac{e}{\epsilon_0}(n_i - n_e), \tag{5.1d}$$

where all quantities are only functions of x and the subscript x is dropped. The force by the ion pressure is ignored by an assumption that the ion temperature is is much smaller than the electron temperature. We normalize eq. (5.1) using units as follows

$$n_i = n_0\tilde{n}_i, \quad u_i = C_s\tilde{u}_i, \quad \phi = \frac{T_e}{e}\tilde{\phi}, \tag{5.2}$$

$$x = \lambda_D\tilde{x}, \quad t = (1/\omega_{pi})\tilde{t} \tag{5.3}$$

where λ_D is the Debye length, ω_{pi} is the ion plasma frequency and C_s is the ion sound wave. And the normalized equations are as follows:

$$\frac{dn_i}{dt} = -n_i\frac{\partial u_i}{\partial x}, \tag{5.4a}$$

$$\frac{du_i}{dt} = -\frac{\partial \phi}{\partial x}, \tag{5.4b}$$

$$\frac{\partial \phi^2}{\partial x^2} = exp(\phi) - n_i. \tag{5.4c}$$

Consider a small perturbations from a uniform equillibrium, $n_0 = 1$, $E_0 = 0$, $u_i = 0$. we assume that perturbations have sinusoidal form, $\sim exp[i(kx - \omega t)]$. By linear analysis, we obtain a linear dispersion relation

$$\omega^2 = \frac{k^2}{1 + k^2}. \tag{5.5}$$

In long wavelength range, eq. (5.5) is approximated as

$$\omega \simeq k - \frac{1}{2}k^2 \tag{5.6}$$

The second term represents the dispersion due to the deviation from the quasi-neutral condition. If a wave is steepened by the inertial term, a region in which the differentiation of variables is large, is created. Then, we can not neglect the term $\partial\phi^2/\partial x^2$, and finally a soliton, balancing nonlinearity and dispersion, is created.

We seek a steady solution (a function of $\xi = x - \lambda t$). We assume boundary conditions as

$$n_i \to 1, \quad \phi \to 0, \quad , \frac{\partial \phi}{\partial \xi} \to 0, \qquad (|\xi| \to \infty). \tag{5.7}$$

Owing to this boundary condition, we can integrate eq. (5.4) as

$$\begin{aligned} \frac{d^2\phi}{d\xi^2} &= exp\phi - \frac{1}{\sqrt{1-\frac{2\phi}{\lambda^2}}} && (5.8) \\ &= = -\frac{d}{d\phi}\left(-\lambda^2\sqrt{1-\frac{2\phi}{\lambda^2}} - exp(\phi)\right) && (5.9) \\ &= -\frac{dV}{d\phi}. && (5.10) \end{aligned}$$

We can understand a qualitative behavior of a solution in terms of an analogy with mechanics. The shecmatic picture of the analogy is shown in Fig. 5.1. Here ξ is the time and ϕ is the coordinate of a particle. A particle starting from $\phi = 0$ at the time $\xi = -\infty$ moves toward the potential well. Then the particle goes to the point, where $\phi = \phi_M$. Then, the particle is reflected and goes toward left side as is the case with going toward right side.

Equation (5.8) can be integrated into another form:

$$\frac{1}{2}\left(\frac{\partial\phi}{\partial\xi}\right)^2 = exp(\phi) + \lambda(\lambda^2 - 2\phi)^{1/2} - (\lambda^2 + 1) \tag{5.11}$$

Setting a value of ϕ at a point, $\partial\phi/\partial\xi = 0$, as ϕ_M,

$$\lambda^2 = \frac{[exp(\phi_M)^2 - 1]^2}{2[exp(\phi_M) - 1 - \phi_M]}. \tag{5.12}$$

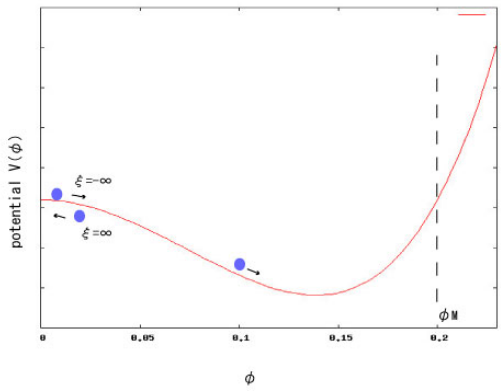

Figure 5.1: Qualitative understanding of the soliton solution in terms of an analogy with a particle motion.

If we assume that an amplitude is much small, i.e., $\phi_M \ll 1$ and $\lambda - 1 = \delta\lambda \ll 1$, eq. (5.11) can be rewritten as

$$\left(\frac{\partial\phi}{\partial\xi}\right)^2 = \frac{2}{3}\phi^2(\delta\lambda - \phi). \tag{5.13}$$

Integration of (5.13) gives the solitary solution

$$\phi = 3\delta\lambda sech^2\left[\left(\frac{\delta\lambda}{2}\right)^{1/2}(x - \lambda t)\right]. \tag{5.14}$$

5.2 SPH equations for ion acoustic wave

SPH equations for ion acoustic wave are obtained just changing the source term of the Poisson equation and the sign of the electric force. In our problem, quasi-particles move along the x-direction at the velocity v_a with charges, the dentisy n_a, the electrostatic potential ϕ_a, the electric field E_a and the mass m_a. Time evolution equations for a particle a are as follows:

$$\frac{dn_a}{dt} = n_a \sum_b \frac{m_b}{n_b}(v_a - v_b)\frac{\partial W_{ab}}{\partial x_a}, \tag{5.15}$$

$$\frac{dv_a}{dt} = E_a, \tag{5.16}$$

$$\frac{dx_a}{dt} = v_a. \tag{5.17}$$

Besides, the electric field carried by the particle a is given by

$$E_a = \sum_b m_b(\phi_a - \phi_b)\frac{\partial W_{ab}}{\partial x_a} \tag{5.18}$$

And the electrostatic potential is obtained by solving

$$\frac{\partial^2 \phi}{\partial x_a^2} = exp(\phi_a) - n_a \tag{5.19}$$

with non-uniform grids distributed on each x_a.

5.3 Poisson solver - Relaxation method -

A difference in the SPH scheme between Langmuir wave and ion acoustic wave is how to solve the Poisson's equation. In the ion acoustic wave, the amplitude of the electric potential has a significant mean, that is, the potential is used in an evaluation of the electrons density, although, in the Langmuir wave, $\boldsymbol{E}$ is just concerned to the physics and we do not care about the absolute value of the potential. Therefore, we have to solve the Poisson equation as a two-point boundary value problem precisely.

We employ a relaxation method to solve the Poisson's equation,

$$\frac{d\phi^2}{dx^2} = exp(\phi_a) - n_a. \tag{5.20}$$

The basic idea of the relaxation method is as follows: Rewrite the equation as a diffusion equation,

$$\frac{\partial \phi}{\partial t} = \frac{d\phi^2}{dx^2} + n_a - exp(\phi_a). \tag{5.21}$$

An initial distribution ϕ_0 relaxes to an equilibrium solution as $t \to \infty$. This equilibrium has all time derivative vanishing. Therefore it is the solution of the original Poisson's equation.

If we use FTCS (Forward Time Central Space) differencing with non-uniform grids, equation (5.21) is discretized for a point j as,

$$\phi_j^{k+1} = \phi_j^k + \Delta t \left(\frac{2\phi_{j-1}^k}{h_1(h_1+h_2)} - \frac{2\phi_j^k}{h_1 h_2} + \frac{2\phi_{j+1}^k}{h_2(h_1+h_2)} + (n_j^k - exp(\phi_j^k)) \right), \tag{5.22}$$

where $h_1 = x_j - x_{j-1}$ and $h_2 = x_{j+1} - x_j$. Subscripts j and k express the grid number in the discretized space and time. In terms of this differentiation, we integrate the equation iteratively. Here we employ the classical Jacobi's method. This method is not practical because it converges too slowly. However, since we don't aim at high speed computation at present, we do not employ faster but complicated iteration method.

5.4 Simulation of linear ion acoustic wave

Before proceeding to a nonlinear simulation, we simulate a one-dimensional linear ion acoustic wave as a bench mark of the numerical scheme. Procedures of the numerical scheme is same as the SPH for Langmuir wave, therefore we do not mention it.

5.4.1 Initial condition and boundary condition

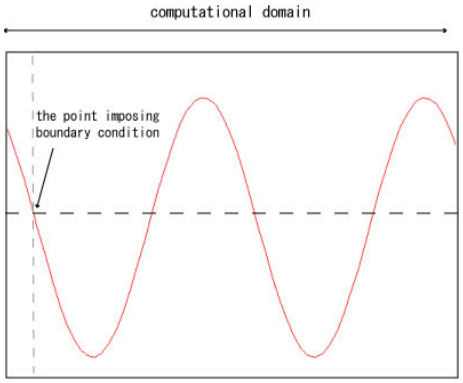

Figure 5.2: How to impose the boundary condition in the Poisson solver: We plotted a density profile in the figure.

Since we want to obtain a dispersion relation of the ion acoustic wave, we input an eigenvectors of ion acoustic wave as an initial condition. Concrete forms of the initial condition are as follows,

$$n_i(x) = 1.0 + 0.01sin(kx), \tag{5.23}$$

$$u_i(x) = \frac{\omega_i}{k}0.01sin(kx), \tag{5.24}$$

$$\phi(x) = \frac{\omega_i}{k}0.01sin(kx), \tag{5.25}$$

where ω_i is the function of k and expressed as

$$\omega_i = \sqrt{\frac{k^2}{1+k^2}}. \tag{5.26}$$

Initial condition for E_x is obtained in the scheme consistently.

We employ a periodic boundary condition as we did in previous chapters. However, here we should mention how to impose the boundary condition in a subroutine solving the Poisson's equation, i.e, where we have to define a two-point boundary value problem.

As shown in Fig. 5.2, the boundary condition $\phi = 0$ is imposed at a point where the density is equal to the equilibrium value. For example, we set the position as x_0. To place the point x_0 at the edge of the computational domain, we introduce a renewed computational domain. In particular, the region to the left of x_0 is attached next to $x = L$, where L is the system size of a computational domain. In terms of updated configuration, we perform the relaxation method and obtain a potential in the updated configuration. Then, we relate values in the updated configuration with values in the original computational domain.

5.4.2 Numerical results

We ran simulations for several waves numbers, such as 2π, 3π and 4π. In Fig. 5.3, propagation of eigenfunctions, initial sinusoidal curve, is demonstrated. In Fig. 5.3, the case where $k = 2\pi$ is plotted. The wave seems to be propagating stably. Error of amplitude per wave period is order of 10^{-4} and this is consistent with a value expected by error estimation.

A dispersion relation derived numerically is shown in Fig. 5.4, with the analytic dispersion relation. We see that the numerical dispersion relation agrees well with the analytic one. Therefore, we assure that SPH for ion acoustic wave works well in linear regime.

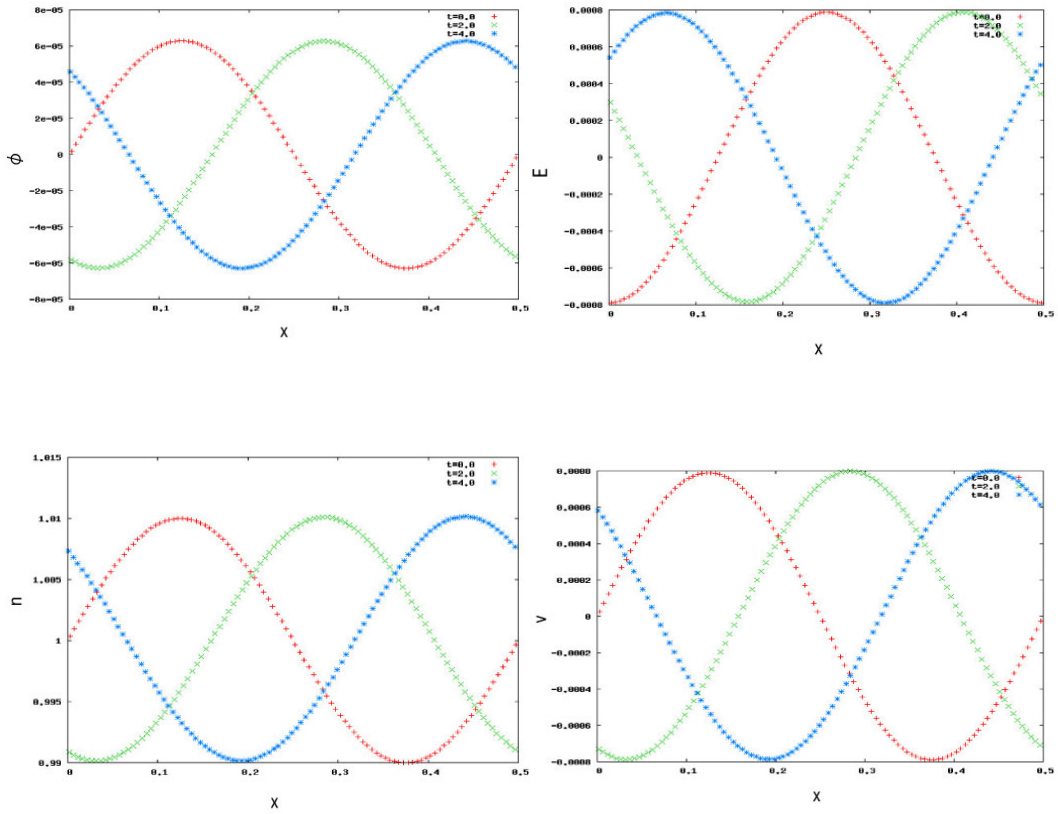

Figure 5.3: The picture of propagating linear ion acoustic wave (k=2π).

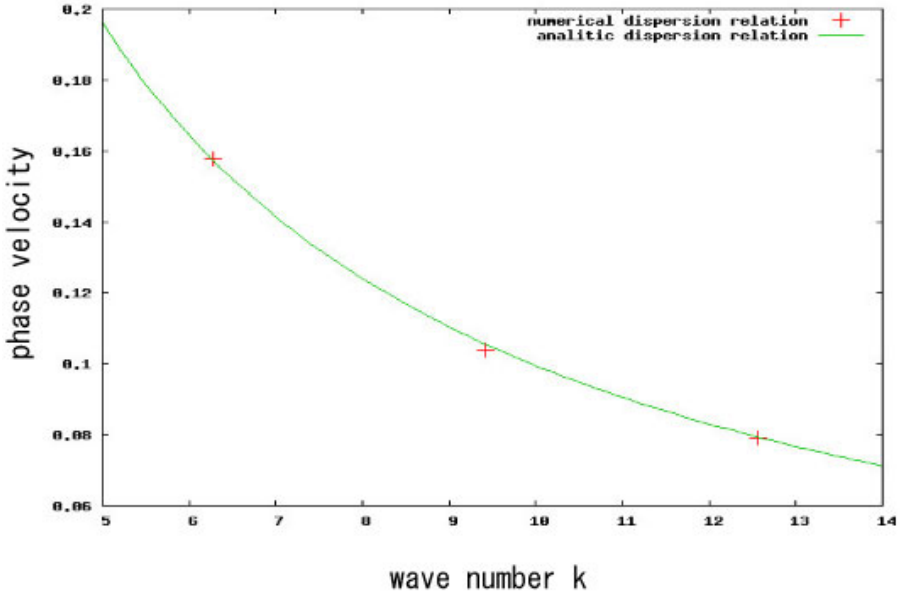

Figure 5.4: Dispersion relation derived numerically and analytically.

5.5 Simulation of nonlinear ion acoustic soliton

Here, we consider a numerical simulation of non-linear ion acoustic soliton. In the conventional SPH, simulation of non-linear wave was performed already, for example, they simulate propagation of water wave, one of the non-linear wave. This is the first SPH simulation of non-linear wave involving plasma physics. We see whether a soliton, initially injected as an analytic solution, propagate stably.

5.5.1 Initial condition and boundary condition

Initial conditions are derived by solving eq. (5.8). At $t = 0$, we can regard ξ as x, since $\xi = x - \lambda t$. We transform the second-order differential equation (5.8) into a pair of first-order differential equations, as

$$\frac{d\phi}{dx} = z, \tag{5.27}$$

$$\frac{dz}{dx} = \exp\phi - \frac{1}{\sqrt{1 - \frac{2\phi}{\lambda^2}}}. \tag{5.28}$$

with initial conditions, $\phi(0) = \phi_M$ and $z(0) = d\phi(0)/dx = 0$. We solve eqs. (5.27)-(5.28) in terms of the fourth-order Runge-Kutta method. Initial profiles of u_i and n_i are obtained from the relation

$$u_i = \lambda - \sqrt{\lambda^2 - 2\phi}, \tag{5.29}$$

$$n_i = \frac{-\lambda}{u_i - \lambda} \tag{5.30}$$

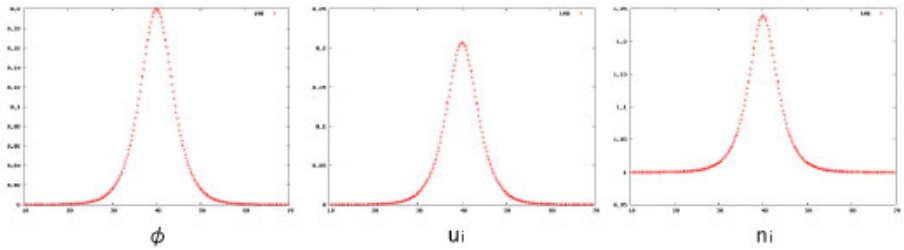

Figure 5.5: A picture of initial profile of ϕ, u_i and n_i .

The initial profile are shown in Fig. 5.5.

We employ periodic boundary here, although the actual system is not periodic. However, since dynamics of interest occurs in the central region of computational domain, unphysical effect due to the inconsistent boundary condition seems to be sufficiently small.

5.5.2 Numerical results

We consider a ion acoustic soliton in a one-dimensional domain, where the system length is 80. We distribute 16000 particles in this computational domain. The time evolution of the soliton is shown in Fig. 5.6. The maximum value of the electric potential is set to be 0.2 initially. We can see that the soliton is propagating stably not changing its profile. To investigate this statement in more detail, we lay the wave form at $t = 6.0$ and $t = 12.0$ on the initial profile. This is shown in Fig. 5.7. Here, we clearly recognize that the soliton is propagating stably. We mention the change of amplitude per $\Delta x/\lambda$, where Δx is the half width of the wave profile. The error of amplitude is less than 1% and this is consistent with the error evaluation.

The wave velocity obtained numerically is 1.07, while the wave velocity expected analitically is 1.14. Therefore, there is the erroness of the order of 5-6%. This value seems to be large compared with the simulation results for the linear wave. Qualitative understanding this situation is as follows: The decrease of the accuracy is originated from the utilization of the uniform smoothing length h, that is, all particle have same h. Accuracy is determined by this smoothing length h, where $h = (m/\rho)^{1/3}$, in the SPH. Therefore, formally, we have to change the smoothing length corresponding to the mass and the mass density carried by the particles. When the nonlinearity is strong, the difference in the density in the central region and in the boundary region increases. Then, Due to the uniform smoothing length, the accuracy decreases. However, the SPH algorithm using inhomogeneous smoothing length is developed in SPH for neutral fluid ([16], [38]). Therefore, we can reduce the error due to the large density difference enhanced by nonlinearity in terms of inhomogeneous smoothing length, although additional computational efforts are needed.

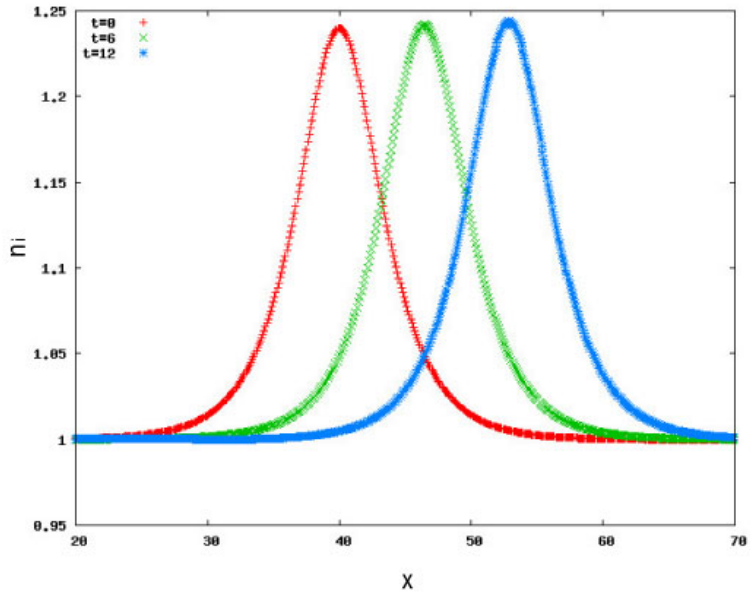

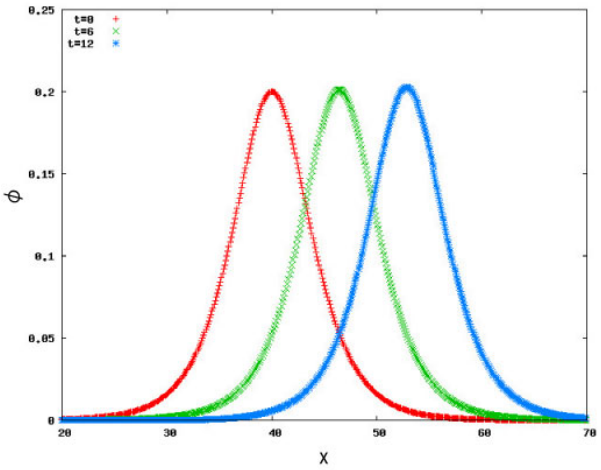

Figure 5.6: Pictures of travelling ion acoustic soliton.

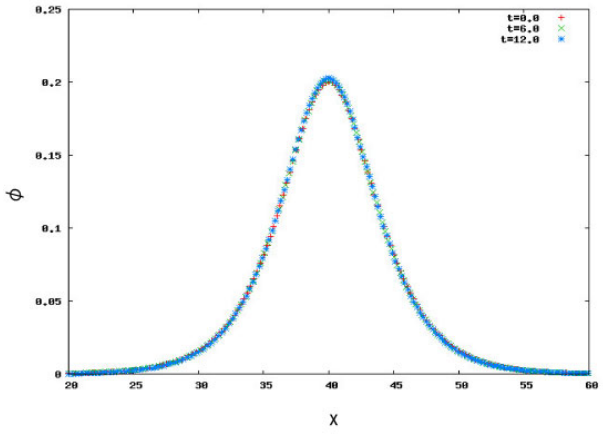

Figure 5.7: To check that the soliton is propagating stably, we lap the profiles at $t = 6$ and 12 over the initial profile. The profiles at $t = 6$ and 12 are shifted in the $-x$-direction by using the propagation velocity obtained numerically.

Chapter 6

Conclusions

In this thesis, we proposed a new multiscale simulation algorithm, called multiscale particle simulation. In the multiscale particle simulation, a multiscale simulation can be performed as follows: Distributed quasi-particles express the characteristics at the level of the scale hierarchy, where they move. Then, quasi-particles change their property depending on the environment. Furthermore, the environment itself is governed by the motion of the quasi-particles. The multiscale particle algorithm can be recognized as a simulation method which incorporates the idea of singular perturbation in the numerical scheme. A schematic understainding of the multiscale particle simulation is shown in Fig. 1.3. A strategy of developing multiscale particle simulation is as follows: At first, we develop numerical schemes in terms of particle method for each model which belongs to the scale hierarchy, that is, we prepare modules for the multiscale particle simulation. After that, we consider connection among the developed particle methods. In the thesis, particularly, we concentrated our attention to the connection between two-fluid model and MHD. The connection of them is the first step of sequencial scale coupling, since two-fluid model lies just below macroscopic MHD model in the scale hierarchy.

In Chap. 2, we clarified the relation of variational principles between MHD and two-fluid model, since the comprehensive understanding of the relation of models can be needed to perform the multiscale simulation. We obtained the equation of motion for MHD, starting from the two-fluid Lagrangian based on the particle's view or an extention of the Lagrangian for the charged particle. In terms of this fact, it can be stated that the particle's

view is essential to the connection of fluid models, and that the multiscale simulation or the scale coupling in the numerical scheme also can be realized in terms of particle's view, i.e., particle method in the terminology of numerical simulation.

In Chap. 3, we developed the Smoothed Particle Hydrodynamics (SPH) method for Hall-MHD which is one of the necessary modules for the multiscale fluid simulation. Since the direct discretization of full Hall-MHD to quasi-particles leads the gyromotion of the quasi-particles, we expect to miss fluid motion of interest and to reduce computational efficiency. Thus, we developed Hall-MHD utilizing drift approximation. We assured that the drift Hall-MHD describe the dispersion relation of shear Alfvén wave well. In terms of the drift Hall-MHD, we developed the SPH for Hall-MHD and simulated 1-D shear Alfvén wave propagating along the magnetic field line. We have confirmed that the dispersion relation obtained numerically agrees well with the analytic one. Therefore, we have succeeded to develop the SPH for Hall-MHD describing shear Alfvén wave, which is one of the most important waves in macroscopic description of plasmas.

In Chap. 4, we considered the SPH which can describe the quasi-particles' motion along the magnetic field line. The SPH for drift Hall-MHD, due to the simple approximation, we did not capture the particles' motion along the magnetic field and neglected the pressure, which characterize the difference between quasi-particles and real particles. Particularly, we developed the SPH for Langmuir wave and observed whether the dispersion due to the pressure is treated properly in terms of numerical simulations. The dispersion relation obtained numerically agrees with the analytic one. Although the error seems to increase as the pressure increases, we found that the error can be reduced by using more smoothed estimationf of the pressure of quasi-particles. Therefore, we have succeeded to develop SPH including the paricles' motion along the magnetic field line.

In Chap. 5, we simulated the ion-acoustice wave to investigate the validity of the developed SPH scheme in the non-linear range. We observed that a solitary solution can propagate stably with no change of its profile. We found the error of the numerical phase velocity compared to the analytic one is of the order of several percents. This is caused by the utilization of uniform smoothing length $h \sim (m/\rho)^{1/3}$ which determines the spatial accuracy. When

nonlinearity increases, the difference of h between particles in the high density region and in the low density region cannot be neglected and the accuracy decreases. We can improve this by introducing variable smoothing length [16]. Therefore, we conclude that the developed SPH scheme can describe the non-linear wave.

In this thesis, we have developed the SPH method for two-fluid model, containing the microscopic length/time scales. We observed that the developed SPH scheme can describe both the transverse wave or motion across the magnetic field lines, and the longitidinal wave or motion along the magnetic field lines, properly. We have developed elementary modules for the multiscale fluid simulation by using particle method, and have investigated the basic features of the modules. Especially, we developed the SPH schemes which can treat the electrostatic dynamics of plasmas and the part of electromagnetic dynamics in which the Hall-effect is important. Combination of the developed SPH scheme will make us to proceed to a new phase of research of multiscale simulation science.

Appendix A

Suppliments to Chapter 2

A.1 Variation of L_{MHD}

Here we consider the variation of $\int L_{MHD}dt$ and derive the equation of motion. The Lagrangian is defined as

$$L_{MHD} = \int (\frac{1}{2}\rho u^2 - \rho\epsilon - \frac{1}{2}B^2)dx^3 \tag{A.1}$$

and variations are as follows:

$$\boldsymbol{x}(\boldsymbol{a}, t) \to \boldsymbol{x}(\boldsymbol{a}, t) + \boldsymbol{\xi}(\boldsymbol{x}, t), \tag{A.2a}$$

$$\delta\boldsymbol{u} = \frac{\partial\boldsymbol{\xi}}{\partial t} + (\boldsymbol{u}\cdot\nabla)\boldsymbol{\xi} - (\boldsymbol{\xi}\cdot\nabla)\boldsymbol{u}, \tag{A.2b}$$

$$\delta\rho = -\nabla(\rho\boldsymbol{\xi}), \tag{A.2c}$$

$$\delta\epsilon = \frac{p}{\rho^2}\delta\rho, \tag{A.2d}$$

$$\delta\boldsymbol{B} = \nabla\times(\boldsymbol{\xi}\times\boldsymbol{B}) \tag{A.2e}$$

Variation of action is given

$$\delta I = \int Ldt = \int \delta L dt, \tag{A.3}$$

which is subjected to the boundary condition, $\boldsymbol{\xi}(t_1) = 0$, $\boldsymbol{\xi}(t_2) = 0$ and $\boldsymbol{\xi}(|\boldsymbol{x}| \to \infty) = 0$. δL_{MHD} is given by,

$$\delta L_{MHD} = \frac{1}{2}\delta\rho u^2 + \rho\boldsymbol{u}\cdot\delta\boldsymbol{u} - \delta\rho\epsilon - \rho\delta\epsilon - \boldsymbol{B}\cdot\delta\boldsymbol{B}. \tag{A.4}$$

Substituting eq. (A.2) into eq. (A.4),

$$\delta I = \int dx^3 dt \Bigg(-\frac{1}{2}u^2 \nabla\cdot(\rho\boldsymbol{\xi}) + \rho\boldsymbol{u}\cdot\left\{\frac{\partial\boldsymbol{\xi}}{\partial t} + (\boldsymbol{u}\cdot\nabla)\boldsymbol{\xi} - (\boldsymbol{\xi}\cdot\nabla)\boldsymbol{u}\right\} + \epsilon\nabla\cdot(\rho\boldsymbol{\xi}) + \frac{p}{\rho}\nabla\cdot(\rho\boldsymbol{\xi}) - \boldsymbol{B}\cdot\{\nabla\times(\boldsymbol{\xi}\times\boldsymbol{B})\}\Bigg) \tag{A.5}$$

We integrate all terms in eq. (A.5) by parts. The first term can be written as,

$$\int dx^3 dt \left\{-\frac{1}{2}u^2\nabla\cdot(\rho\boldsymbol{\xi})\right\} = \int dx^3 dt \left\{-\frac{1}{2}u^2\frac{\partial}{\partial x^i}(\rho\xi^i)\right\} \tag{A.6}$$

$$= \int dx^3 dt \left\{-\frac{\partial}{\partial x^i}\left(\frac{1}{2}\rho u^2\xi^i\right) + \rho\xi^i\frac{\partial}{\partial x^i}(\frac{u^2}{2})\right\} \tag{A.7}$$

$$= \int dx^3 dt \left\{\rho\xi^i\frac{\partial}{\partial x^i}(\frac{u^2}{2})\right\}. \tag{A.8}$$

Here, we omitted the divergence term because of the boundary condition. Here after, although we drop the symbol $\int dx^3 dt$ for simple notation, the divergence term is dropped by the boundary condition for time and space. For the second term,

$$\rho\boldsymbol{u}\cdot\frac{\partial\boldsymbol{\xi}}{\partial t} = \frac{\partial}{\partial t}(\rho u^i\xi^i) - \xi^i\frac{\partial}{\partial t}(\rho u^i) \tag{A.9}$$

$$= -\xi^i\frac{\partial}{\partial t}(\rho u^i). \tag{A.10}$$

The third term and fourth term are written as

$$\rho u^i u^j\frac{\partial\xi^i}{\partial x^j} = \frac{\partial}{\partial x^j}\left(\rho u^i u^j\xi^i\right) - \xi^i\frac{\partial}{\partial x^j}\left(\rho u^i u^j\right) \tag{A.11}$$

$$= -\xi^i\frac{\partial}{\partial x^j}\left(\rho u^i u^j\right), \tag{A.12}$$

$$-\rho\boldsymbol{u}\cdot\{(\boldsymbol{\xi}\cdot\nabla)\boldsymbol{u}\} = -\xi^i\rho u^j\frac{\partial u^j}{\partial x^i} \tag{A.13}$$

$$= -\boldsymbol{\xi}\cdot\rho\nabla\frac{u^2}{2}, \tag{A.14}$$

respectively. In the same way, the fifth and sixth term also can be written as

$$(\epsilon + \frac{p}{\rho})\nabla\cdot(\rho\boldsymbol{\xi}) = -\rho\xi^i\frac{\partial}{\partial x^i}(\frac{p}{\rho} + \epsilon) \tag{A.15}$$

$$= -\rho\xi^i(\frac{1}{\rho}\frac{\partial p}{\partial x^i} - \frac{p}{\rho^2}\frac{\partial\rho}{\partial x^i} + \frac{p}{\rho^2}\frac{\partial\rho}{\partial x^i}) \tag{A.16}$$

$$= -\boldsymbol{\xi}\cdot\nabla p, \tag{A.17}$$

where, we use the relation $\partial\epsilon/\partial\rho = p/\rho^2$. The last term is written as,

$$\begin{aligned}
-\boldsymbol{B}\cdot(\nabla\times(\boldsymbol{\xi}\times\boldsymbol{B})) &= -\boldsymbol{B}\cdot\{\boldsymbol{\xi}(\nabla\cdot\boldsymbol{B}-\boldsymbol{B}(\nabla\cdot\boldsymbol{\xi})+(\boldsymbol{B}\cdot\nabla)\boldsymbol{\xi}-(\boldsymbol{\xi}\cdot\nabla)\boldsymbol{B}\} \\
&= B^i(B^i\frac{\partial\xi^j}{\partial x^j}-B^j\frac{\partial\xi^i}{\partial x^j}+B^i\xi^j\frac{\partial B^i}{\partial x^j}) \\
&= -\xi^i\frac{\partial}{\partial x^i}(\frac{B^2}{2}+B^j\frac{\partial B^i}{\partial x^j} \\
&= \boldsymbol{\xi}\cdot\left(-\nabla\frac{B^2}{2}+(\boldsymbol{B}\cdot\nabla)\boldsymbol{B}\right) \\
&= \boldsymbol{\xi}\cdot(\boldsymbol{j}\times\boldsymbol{B}) \qquad \text{(A.18)}
\end{aligned}$$

Collecting the remaining terms,

$$\boldsymbol{\xi}\cdot\left\{\rho\nabla\frac{u^2}{2}-\frac{\partial}{\partial t}(\rho\boldsymbol{u})-\nabla(\rho\boldsymbol{u}\boldsymbol{u})-\rho\nabla\frac{u^2}{2}-\nabla p+\boldsymbol{j}\times\boldsymbol{B}\right\} \quad \text{(A.19)}$$

$$=\boldsymbol{\xi}\cdot\left\{-\frac{\partial\rho}{\partial t}\boldsymbol{u}-\rho\frac{\partial\boldsymbol{u}}{\partial t}-\rho(\boldsymbol{u}\cdot\nabla)\boldsymbol{u}-\boldsymbol{u}(\nabla\cdot\rho\boldsymbol{u})-\nabla p+\boldsymbol{j}\times\boldsymbol{B}\right\}, \quad \text{(A.20)}$$

$$=\boldsymbol{\xi}\cdot(-\rho\frac{\partial\boldsymbol{u}}{\partial t}-\rho(\boldsymbol{u}\cdot\nabla)\boldsymbol{u}-\nabla p+\boldsymbol{j}\times\boldsymbol{B}) \quad \text{(A.21)}$$

If we set eq. (A.21) to be zero, we derive the equation of motion,

$$\rho\left(\frac{\partial\boldsymbol{u}}{\partial t}+(\boldsymbol{u}\cdot\nabla)\boldsymbol{u}\right)=-\nabla p+\boldsymbol{j}\times\boldsymbol{B}. \qquad \text{(A.22)}$$

A.2 Variation of L_i

Here we consider the variation of $\int L_i dt$ and derive the equation of motion for ions. The Lagrangian for ion fluid is defined as

$$L_i=\int dx^3(\frac{1}{2}\rho u^2-\rho\epsilon+en\boldsymbol{u}\cdot\boldsymbol{A}-en\phi), \qquad \text{(A.23)}$$

and variations are given as

$$\boldsymbol{x}(\boldsymbol{a},t)\rightarrow\boldsymbol{x}(\boldsymbol{a},t)+\boldsymbol{\xi}(\boldsymbol{x},t), \qquad \text{(A.24)}$$

$$\delta\rho=-\nabla\cdot(\rho\boldsymbol{\xi}), \qquad \text{(A.25)}$$

$$\delta\boldsymbol{u}=\frac{\partial\boldsymbol{\xi}}{\partial t}+(\boldsymbol{u}\cdot\nabla)\boldsymbol{\xi}-(\boldsymbol{\xi}\cdot\nabla)\boldsymbol{u}, \qquad \text{(A.26)}$$

$$\delta\epsilon=\frac{\partial\epsilon}{\partial\rho}\delta\rho=\frac{p}{\rho}\delta\rho, \qquad \text{(A.27)}$$

$$\delta\boldsymbol{A}=0,\quad \delta\boldsymbol{\phi}=0, \qquad \text{(A.28)}$$

where we omitt the subscript i for simplicity. Sunstituting (A.24)-(A.28) into (A.23), the variation of action is given by

$$\delta I = \int dtdx^3 \{ -\frac{u^2}{2}\nabla\cdot(\rho\boldsymbol{\xi}) + \rho\boldsymbol{u}\cdot\big(\frac{\partial\boldsymbol{\xi}}{\partial t} + (\boldsymbol{u}\cdot\nabla)\boldsymbol{\xi} - (\boldsymbol{\xi}\cdot\nabla)\boldsymbol{u}\big) - e(\boldsymbol{u}\cdot\boldsymbol{A})\nabla\cdot(n\boldsymbol{\xi}) + en\boldsymbol{A}\cdot\big(\frac{\partial\boldsymbol{\xi}}{\partial t} + (\boldsymbol{u}\cdot\nabla)\boldsymbol{\xi} - (\boldsymbol{\xi}\cdot\nabla)\boldsymbol{u}\big) + e\phi\nabla\cdot(n\boldsymbol{\xi}) + \epsilon\nabla\cdot(\rho\boldsymbol{\xi}) + \frac{p}{\rho}\nabla\cdot(\rho\boldsymbol{\xi})\,\}\,. \tag{A.29}$$

We integrate all terms in (A.29) by parts. Transformation of first four terms and last two terms is the same calculated in Appendix A. Therefore we consider a transformation of rest terms in (A.29). The fifth term can be rewritten as

$$-e(\boldsymbol{u}\cdot\boldsymbol{A})\nabla\cdot(n\boldsymbol{\xi}) = -eu^jA^j\frac{\partial}{\partial x^i}(n\xi^i) \tag{A.30}$$

$$= -e\frac{\partial}{\partial x^i}(u^jA^jn\xi^i) + en\xi^i\frac{\partial}{\partial x^i}(A^ju^j) \tag{A.31}$$

$$= \boldsymbol{\xi}\cdot\big[en\nabla(\boldsymbol{A}\cdot\boldsymbol{u})\big], \tag{A.32}$$

where we omitt the symbol $\int dtdx^3$ for simple notation and drop the surface integral in terms of boundary conditions. The next term $en\boldsymbol{A}\cdot\frac{\partial\boldsymbol{\xi}}{\partial t}$ can be written as

$$enA^i\frac{\partial\xi^i}{\partial t} = \frac{\partial}{\partial t}(enA^i\xi^i) - e\xi^i\frac{\partial n}{\partial t}A^i - en\xi^i\frac{\partial A^i}{\partial t} \tag{A.33}$$

$$= \boldsymbol{\xi}\cdot\left[-e\frac{\partial n}{\partial t}\boldsymbol{A} - en\frac{\partial\boldsymbol{A}}{\partial t}\right]. \tag{A.34}$$

Next term is written as

$$en\boldsymbol{A}\cdot[(\boldsymbol{u}\cdot\nabla)\boldsymbol{\xi}] = enA^iu^j\frac{\partial}{\partial x^j}\xi^i \tag{A.35}$$

$$= \frac{\partial}{\partial x^j}(enA^iu^j\xi^i) - \xi^i\frac{\partial}{\partial x^j}(enA^iu^j) \tag{A.36}$$

$$= -\boldsymbol{\xi}\cdot[e\boldsymbol{A}(\nabla\cdot n\boldsymbol{u}) + en(\boldsymbol{u}\cdot\nabla)\boldsymbol{A}]\,. \tag{A.37}$$

Next term can be written in terms of another notation as

$$-en\boldsymbol{A}\cdot[(\boldsymbol{\xi}\cdot\nabla)\boldsymbol{u}] = -en\boldsymbol{\xi}\cdot[\nabla\boldsymbol{u}\cdot\boldsymbol{A}], \tag{A.38}$$

where $\nabla \boldsymbol{u}$ is a matrix, its (i,j) componets is expressed as $\partial u^j/(\partial x^i)$. Finally,

$$e\phi \nabla \cdot (n\boldsymbol{\xi}) = e\phi \frac{\partial}{\partial x^i}(n\xi^i) \tag{A.39}$$

$$= \frac{\partial}{\partial x^i}(e\phi n \xi^i) - en\xi^i \frac{\partial \phi}{\partial x^i} \tag{A.40}$$

$$= \boldsymbol{\xi} \cdot (-en\nabla\phi) \tag{A.41}$$

Collecting all terms, eq. (A.29) can be written as

$$\delta I = \int dt dx^3 \boldsymbol{\xi} \cdot \Bigg[-\rho \frac{\partial \boldsymbol{u}}{\partial t} - \rho(\boldsymbol{u}\cdot\nabla)\boldsymbol{u} - \nabla p + en\nabla(\boldsymbol{A}\cdot\boldsymbol{u}) - en(\frac{\partial \boldsymbol{A}}{\partial t} + \nabla\phi)$$
$$-e\boldsymbol{A}(\frac{\partial n}{\partial t} + \nabla(n\boldsymbol{u})) - en(\boldsymbol{u}\cdot\nabla)\boldsymbol{A} - en(\nabla\boldsymbol{u})\cdot\boldsymbol{A} \Bigg]. \tag{A.42}$$

We use the continuity equation and the vector identity,

$$\frac{\partial}{\partial x^i}(A^j u^j) - u^j \frac{\partial A^i}{\partial x^j} - A^j \frac{\partial u^j}{\partial x^i} = [\boldsymbol{u} \times (\nabla \times \boldsymbol{A})]^i. \tag{A.43}$$

Then, we obtain

$$\rho \frac{d\boldsymbol{u}}{dt} = en(\boldsymbol{E} + \boldsymbol{u} \times \boldsymbol{B}) - \nabla p \tag{A.44}$$

A.3 Variation of Lagrangian (2.69)

Here we mention the supplimental calculations to the context of Sec. 2.3.3. We consider the variation of the Lagrangian (2.69). Concerned variations are as follows:

$$\boldsymbol{x}(\boldsymbol{a}, t) \to \boldsymbol{x}(\boldsymbol{a}, t) + \boldsymbol{\xi}(\boldsymbol{x}, t), \tag{A.45}$$

$$\delta\rho = -\nabla\cdot(\rho\boldsymbol{\xi}), \tag{A.46}$$

$$\delta A = 0, \tag{A.47}$$

$$\delta\boldsymbol{u} = \frac{\partial \boldsymbol{\xi}}{\partial t} + (\boldsymbol{u}\cdot\nabla)\boldsymbol{\xi} - (\boldsymbol{\xi}\cdot\nabla)\boldsymbol{u}, \tag{A.48}$$

$$\delta\boldsymbol{j} = \nabla \times (\boldsymbol{\xi} \times \boldsymbol{j}). \tag{A.49}$$

Actually most of calculation are the same in the case of variational principle of MHD. A difference appears in the variation of the current density. Therefore, we see transformation of the term involving the variation of the current

density.

$$\boldsymbol{A} \cdot [\nabla \times (\boldsymbol{\xi} \times \boldsymbol{j})] = A^i \epsilon^{ijk} \frac{\partial}{\partial x^j} \epsilon^{klm} \xi^l j^m \tag{A.50}$$

$$= \frac{\partial}{\partial x^j} (\epsilon^{ijk} \epsilon^{klm} A^i \xi^l j^m) - \epsilon^{kij} \epsilon^{klm} \xi^l j^m \frac{\partial A^i}{\partial x^j} \tag{A.51}$$

$$= (\delta_{im}\delta_{jl} - \delta_{il}\delta_{jm}) \xi^l j^m \frac{\partial A^i}{\partial x^j} \tag{A.52}$$

$$= \xi^i \left[j^m \frac{\partial A^m}{\partial x^i} - j^m \frac{\partial A^i}{\partial x^m} \right] \tag{A.53}$$

$$= \boldsymbol{\xi} \cdot (\boldsymbol{j} \times (\nabla \times \boldsymbol{A})) \tag{A.54}$$

$$= \boldsymbol{\xi} \cdot (\boldsymbol{j} \times \boldsymbol{B}), \tag{A.55}$$

where we use the identity

$$A^j \left(\frac{\partial B^j}{\partial x^i} - \frac{\partial B^i}{\partial x^j} \right) = [\boldsymbol{A} \times (\nabla \times \boldsymbol{B})]^i \tag{A.56}$$

We can derive the Lorentz force $\boldsymbol{j} \times \boldsymbol{B}$ apparently.

Bibliography

[1] J. P. Freidberg, *Ideal Magnetohydrodynamics* (Prenum Press).

[2] H. Goedbloed, *Principles of Magnetohydrodynamics* (Cambridge University Press, 2003).

[3] S. Chapman and T. G. Cowlin, *The Mathematical Theory of Non-uniform Gases*, (Cambridge University Press, 1970)

[4] S. I. Braginskii, *Reviews of Plasma Physics Vol. I* (1965).

[5] R. Balescu, *Transport Processes in Plasmas*(Amsterdam, North Holland, 1988).

[6] D. Biskamp, *Magnetic Reconnection in Plasmas* (Cambridge University Press, 2000).

[7] E. R. Priest and T. Forbes, *Magnetic Recconection* (Cambridege University Press, 2000).

[8] E. N. Parker, Astrophys. J. **471**, 489 (1996); E. N. Parker, *Spontaneous Current Sheets in Magnetic Fields* (Oxford, 1994).

[9] S. M. Mahajan and Z. Yoshida, Phys. Rev. Lett. **81**, 4863 (1998).

[10] Z. Yoshida and S. M. Mahajan, Phys. Rev. Lett. **88**, 095001 (2002).

[11] V. I. Arnold, *Mathematical Methods of Classical Mechanics* (Springer, 1978).

[12] R. J. Goldston and P. H. Rutherford, *Introduction to Plasma Physics* (IOP, 1995).

[13] R. Numata, *Ph.D thesis* (Univ. of Tokyo, 2003).

[14] C. K. Birdsall, *Plasma Physics via Computer Simulation*, (Bristol, 1991).

[15] J. J. Monaghan, Ann. Rev. Astron. Astrophys., **30**, 543.

[16] J. J. Monaghan, D. J. Price, MNRAS **350**, 1449.

[17] P. J. Morrison, Rev. Mod. Phys. **70**, 467.

[18] R. Salmon, Annual Review of Fluid Mechanics, **20**, 225.

[19] G. B. Whitham, *Linear and Nonlinear Waves* (Wiley, 1974).

[20] J. R. Cary, Phys. Rep. **79**, 129 (1981).

[21] J. R. and R. G. Littlejohn, Ann. Phys. **151**, 1 (1983)

[22] R. G. Littlejohn, J. Plasma Phys. **29**, 111 (1983)

[23] M. D. Kruskal and C. Oberman, Phys. Fluids **1**, 275 (1958)

[24] T. Taniuchi and K. Nishihara, *Hisenkei hadou* (Iwanami, 1977)

[25] N. A. Krall and A. W. Trivelpiece *Principles of Plasma Physics* (McGraw-Hill, 1973)

[26] R. D. Hazeltine and F. L. Waelbroeck *The Framework of Plasma Physics* (Westview, 2004)

[27] D. Biskamp, *Nonlinear Magnetohydrodynamics*, (Cambridge Univercity Press, 1993)

[28] G. R. Liu and M. B. Liu, *Smoothed Particle Hydrodynamics* (World Scientific, 2003)

[29] J. Birn, J. Drake., M. Shay, B. Rogers, R. Denton, M. Hesse, M. Kuznetsova, Z. Ma, A. Bhattacharjee, A. Otto, *et. al.*, J. Geophys. Res. **106**, 3715 (2001)

[30] K. Kusano, T. Sugiyama, *et. al.*, *Annual Report of the Earth Simulator Center April 2005-March 2006* (The Earth Simulator, 2007)

[31] H. Goldstein, *Classical Mechanics*, (Addison-Wesley, 1980)

[32] C. Eckart, Phys. Fluids **3**, 421 (1960)

[33] C. C. Lin, *Proc. Int. Sch. Phys. XXI*, 93 (New York, Academic, 1963)

[34] R. L. Seliger and G. B. Whitham, Proc. R. Soc. London Ser. A, **305**, 1 (1968)

[35] J. Serrin, *Handbuch der Physik VIII-1*, 125 (Berlin, Springer, 1959)

[36] L. B. Lucy, Astron. J. **82**, 1013 (1977)

[37] R. A. Gingold and J. J. Monaghan, MNRAS **181**, 375 (1977)

[38] W. Benz, *The numerical modelling of nonlinear stellar pulsations*, (Kluwer, Dordrecht, 1990)

Acknowledgement

First of all, I would like to express my gratitude to Professor Zensho Yoshida. His insightful comments based on very wide and deep knowledge about science, not limited to plasma physics and mathematical physics, helped my understanding. Furthermore, he indicated what the physicist is supposed to be about.

I also appreciate Associate Prof. Masaru Furukawa for his kind guidance. I never forget the days, that I developed my simulation code in his office. I learned from him how to proceed the study step-by-step and have increased what I can do thanks to him.

I am grateful to Prof. Yuichi Ogawa and Mr. Junji Morikawa for his kindness. They call to me in a familiar way, whenever. I would like to express my appreciation to Prof. Vazha Berezhiani. He gave me a lot of interesting storys as well as scientific knowledge. And discussions with him in English improved my English.

I am also grateful to Mrs. Nami Sugimura. I look forward to go to the university on Monday, Wednesday and Thursday, especially. The days, which I did not expect the visit of her, are like spectacles. I really take an easy by the chatter with her. I would like to appreciate to all other members in the laboratory.

I was really yankee student for one or two years ago. I caused too many troubles to the colleagues of the laboratory. I would like to give something back to the members as possible as I can in the coming Ph. D life. Finally, I would like to appreciate to the wind blowing in the Kashiwanoha Campus, which blows my depressive emotion away.

研究発表

学会発表

1. 沼澤 修平, 吉田 善章, MHD のラグランジアン形式, 日本物理学会, 2005 年 9 月　(同志社大学)

2. 沼澤 修平, 吉田 善章, 古川 勝, 二流体モデルの Smoothed Particle Hydrodynamics 法, 2006 年 9 月　(千葉大学)